3

Molecular Mechanism of Huntington's Disease — A Computational Perspective

Giulia Rossetti[1] and Alessandra Magistrato[2]
[1]*German Research School for Simulation Science, FZ-Juelich and RWTH,*
[2]*CNR-IOM-National Simulation Center c/o,*
International School for Advanced Studies (SISSA/ISAS), Trieste,
[1]*Germany*
[2]*Italy*

1. Introduction

1.1 The Huntington's Disease

Huntington's Disease (HD) is a devastating autosomal dominant[a] neurodegenerative human disease for which there is currently no cure. HD is characterized by progressive motor, cognitive, and psychiatric symptoms (Huntington 1872). The gene responsible for HD (HTT) encodes the ubiquitously expressed Huntingtin protein (Htt) (MacDonald et al. 1993) (Fig. 1). Human Htt is essential for brain development (Reiner et al. 2003), although its exact biological function is unknown. This protein is located mostly in the cytoplasm, but a small amount of Htt is also present in the nucleus (Kegel et al. 2002). Moreover, the protein can dynamically travel back and forth between the two cellular compartments (Kegel et al. 2002). Htt may be associated also with the plasma membrane, the endocytic and autophagic vesicles, the endosomal compartments, the endoplasmic reticulum, the Golgi apparatus, mitochondria and microtubules (Kegel et al. 2002; Caviston et al. 2007; Kegel et al. 2005; Rockabrand et al. 2007; Strehlow et al. 2007; Atwal et al. 2007). Htt is a large, multidomain protein (3144 aa and molecular weight 348 kDa) for which structural information at atomic resolution is not available (Zuccato et al. 2010). Htt has been proposed to be an elongated super-helical solenoid with a diameter of ~ 200 Å (Li et al. 2006) (Fig. 1). The best-characterized part of the protein is the Exon 1 (Ex1), which consists of the following regions: N17 (the 17-amino acid-long N-term), the variable polyQ stretch (less than 36 Qs in healthy individuals (Mangiarini et al. 1996)), and a polyProline (polyP)-rich region (Fig. 1). Ex1, with an extended polyQ tract (m-Ex1), is sufficient to cause HD-like pathology in animal models (Mangiarini et al. 1996). Moreover, expression of m-Ex1 is sufficient to cause the typical formation of Htt aggregates found in brains of HD patients (Mangiarini et al. 1996; Bates et al. 1998; Davies et al. 1997). Hence, investigations of structural, dynamical and kinetic properties of m-Ex1 may help to understand key aspects of the disease. The amino acids of N17 are highly conserved (100% similarity) in all vertebrate species (Tartari et al. 2008), and

[a]Autosomal dominant conditions are achieved in cases in which a mutated gene from one parent is sufficient to cause a disease, in spite of the presence of a normal gene inherited from the other parent

N17 was originally believed to be unstructured (Perutz 1999). However, mutational analysis *in vivo* and Circular Dicroism (CD) (Atwal et al. 2007; Thakur et al. 2009) spectroscopy and NMR (Thakur et al. 2009) on peptides *in vitro* pointed out that this polypeptide may be an amphipathic α-helix with membrane-associating properties with respect to the endoplasmic reticulum (Atwal et al. 2007). The polyQ stretch begins at the 18th amino acid in human Htt (MacDonald et al. 1993).[b]

In 1994, Max Perutz (Perutz 1994) suggested, for the first time, that the physiological function of polyQ was to bind transcription factors containing also a polyQ region. Consistently, it was later shown that the polyQ tract is a key regulator of Htt binding to its partners (Harjes & Wanker, 2003). This hypothesis is supported by the presence of HEAT repeats (Fig. 1) along the Htt sequence, which favor protein-protein interactions (Andrade & Bork 1995). Moreover, the polyQ region may have flexible and multifunctional structures, which can assume specific conformations and different activities, depending on its binding partners, on its sub-cellular location, and on time of maturation in a given cell type and tissue (Kim et al. 2009; Zuccato et al. 2010).

The polyQ region is followed by a polyP tract (Tartari et al. 2008). This latter may affect the stability of the polyQ segment by keeping it soluble (Bhattacharyya et al. 2006; Steffan et al. 2004). Hence, it may protect polyQ against its conformational collapse. In addition, the polyP may also work also as a protein-interaction domain. Consistent with these hypotheses, structural data provided hints that the polyQ's aggregation and toxicity are influenced by the COOH-terminal polyP region (Kim et al. 2009; Bhattacharyya et al. 2006).

1.2 Mutated huntingtin in HD and the role of polyQ

The causative mutation of Htt is an abnormal expansion of CAG trinucleotide repeats within the coding sequence of the gene. The expansion leads to an elongated stretch of Q residues beyond the first 17 amino acids (MacDonald et al. 1993). In healthy individuals the number of Qs repeats is 35 or fewer, with 17–20 repeats found most commonly (Myers 2004; Housman 1995; Leavitt et al. 1999; Leavitt et al. 2001).[c]

Most adult-onset HD cases feature a mutated form of the protein (m-Htt) with 40–50 Qs. Expansions of 50 and more repeats generally cause the juvenile form of the disease (Gusella & MacDonald 2000). There is a strong negative correlation between the age of HD's onset and the number of Qs (Gusella & MacDonald 2000). Usually, the longer is the polyQ tract, the earlier is the age of the onset (Ross 1995; Gusella & MacDonald 2000). However, for a

[b]In 2008, the first Htt orthologs multi-alignment provides evidence that the polyQ is an ancient acquisition of Htt (Tartari et al. 2008). Its appearance dates back to sea urchin in which a NHQQ sequence is present, which consists of a group of four hydrophilic amino acids that can be considered bio-chemically comparable to the four glutamines (QQQQ) found in fish, amphibians, and birds (Tartari et al. 2008). The polyQ has then expanded gradually in mammals to become the longest and most polymorphic polyQ in humans (Tartari et al. 2008). One possible hypothesis is that wild-type Htt function, during development, may arise from the binding of different sets of interactors: many proteins in the cells contain a polyQ tract, in particular transcription factors and transcriptional regulators (Cha 2007).

[c]Repeats between 27 and 35 are rare and are not associated with disease. However, they are meiotically unstable and can expand into the disease range of 36 and above, when transmitted through the paternal line. Incomplete penetrance has been observed in individuals with 36– 41 repeats, but the estimates of penetrance for this group are imprecise.

given Q length there is a large variation in the age of onset, and the number of Qs by itself has poor predictive power on the age of HD's onset (Imarisio et al. 2008). m-Htt abnormally interacts with other proteins (Sapp et al. 1999) and causes brain damage (Borrell-Pages et al. 2006) producing oxidative stress, excitotoxic processes and metabolism deregulation (Grunewald & Beal 1999; Sapp et al. 1999).[d]

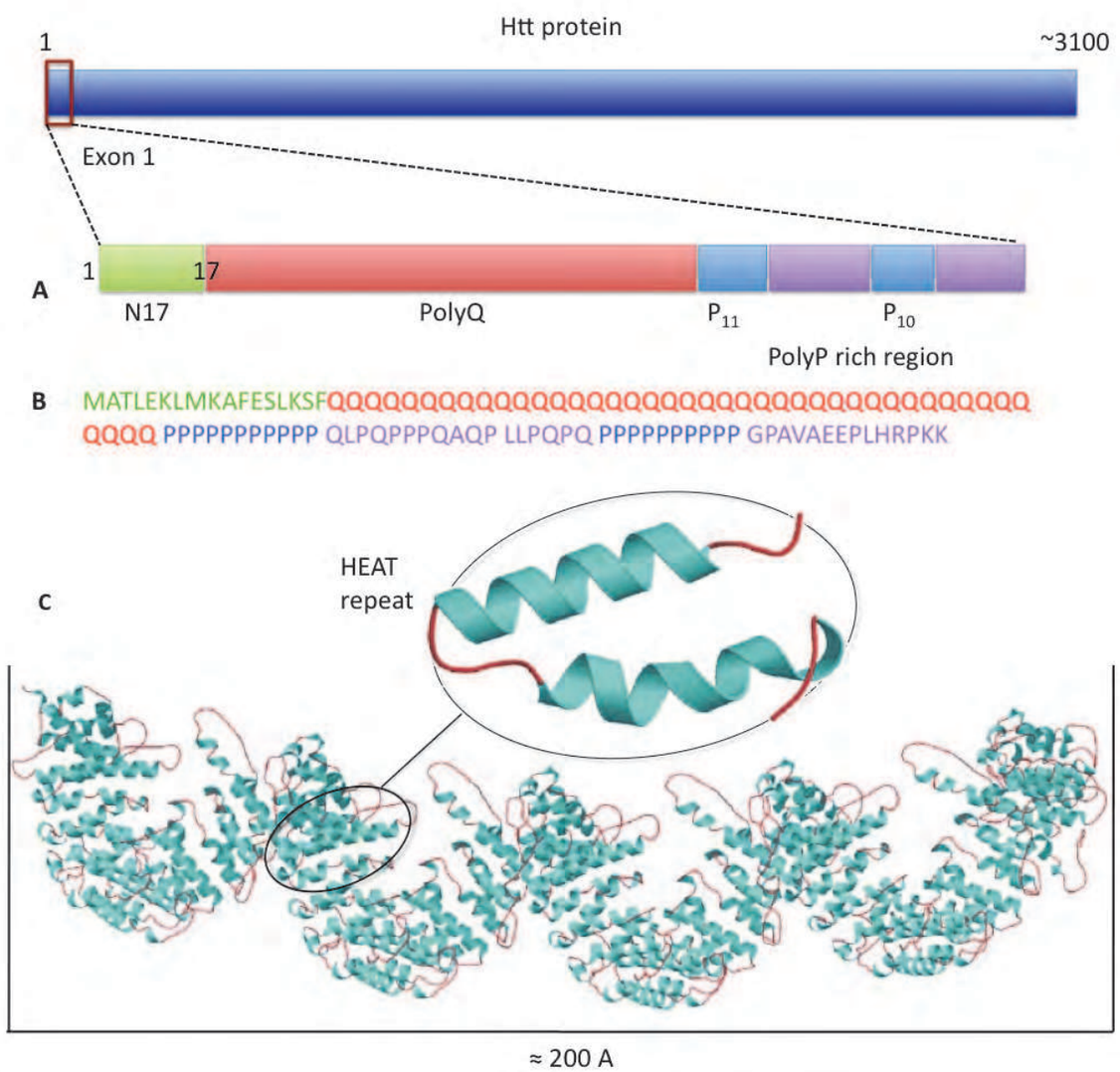

Fig. 1. Htt and Ex1: A) Scheme of Ex1 regions with B) the corresponding primary sequence; C) Proposed model of Htt. The HEAT domain is magnified. HEAT repeats are ~40 amino-acid domains, which fold in two anti-parallel α-helices forming a hairpin (Palidwor et al. 2009). Htt features 16 of these repeats (Andrade & Bork 1995; Palidwor et al. 2009; Li et al. 2006) organized in 4 clusters (Tartari et al. 2008).

[d]The expression of long Q tracts alone, in the context of an N-terminal fragment or full-length Htt protein was shown to disrupt a wide variety of biological functions in cells and model organisms (Johnson and Davidson 2010; Mangiarini et al. 1996; Zoghbi and Orr 2000).

Neuronal intra-nuclear and intra-cytoplasmic inclusions rich in polyQs are the pathological hallmarks of HD (Davies et al. 1997; Trottier et al. 1995). Inclusions are believed to be toxic since they can provoke a physical block of axonal transport between the cell body and the synaptic terminal as well as the recruitment of other polyQ-containing proteins, mainly transcription factors. These latter, interacting with m-Htt, may lose their physiological function, leading to cell death (Gunawardena et al. 2003; Lee et al. 2004; Li et al. 2001; Parker et al. 2001). However, inclusions may also result from an attempt of the cells to proteolytically degrade or inactivate m-Htt (Kuemmerle et al. 1999; Saudou et al. 1998). This alternative proposal is supported by the fact that cells forming Htt inclusions have an improved survival with respect to those not forming them (Arrasate et al. 2004). Accordingly, there is little correlation between inclusions burden and the areas of the brain most affected in HD (Gutekunst et al. 1999; Kuemmerle et al. 1999). The formation of polyQ rich inclusions proceeds through steps that generate different aggregated species, whose populations and stabilities may increase with polyQ length (Bulone et al. 2006). Among these different species are the nuclei, the oligomers, the protofibrils and, finally, the large fibers, which form the microscopic aggregates found in neurons (Ross & Poirier 2004). Unfortunately, the exact degree of toxicity of each species is not known.

Few information is available for protofibrils and fibers (Zuccato et al. 2010), while several efforts were been done to characterize oligomeric species. Indeed, oligomers may be highly reactive toward cellular environment because they have a large surface area with respect to volume ratios, as compared with larger inclusions. This reactivity may be correlated with toxicity (Ross & Poirier 2004; Ross & Poirier 2005; Nagai et al. 2007; Truant et al. 2008). Recent studies highlighted that the oligomers could be formed in several ways such as via N-terminal or direct polyQ interactions (Legleiter et al. 2010; Olshina et al. 2010; Ramdzan et al. 2010). However, the oligomers may also not be the pathway thought which the formation of polyQ larger inclusions takes place (Ross & Tabrizi 2011).

1.3 Role of the flanking regions

N17 and polyP modulate toxicity of m-Htt Ex1 (Truant et al. 2008; Atwal et al. 2007; Bhattacharyya et al. 2005).[e] Indeed, deletion of the proline-rich (P-rich) region in m-Ex1 fragments greatly increases their toxicity in yeast. These m-Ex1 fragments are otherwise innocuous (Dehay & Bertolotti 2006). Therefore, the P-rich region appears to be protective against the effects of expanded polyQ (Bhattacharyya et al. 2005).

N17, present in all mouse models of HD, was shown to modulate the toxicity of m-Htt in a structure-dependent manner (Truant et al. 2008; Atwal et al. 2007). A single point mutation in the middle of N17 was shown to disrupt the possibility to obtain a helical structure, completely abrogating any visible aggregates of m-Htt (Truant et al. 2008; Atwal et al. 2007). Indeed, the initial phases of the aggregation process seem to be accelerated by hydrophobic

[e]Also sequences exogenous to Ex1 modulate aggregation. In the yeast toxicity model, the positioning of flag-tags on the expression constructs modulate toxicity and the nature of aggregated protein (Duennwald et al. 2006). Another group observed modulation of polyQ aggregation by the use of structured chimeras with the cellular retinoic-acid binding protein in *E. coli* (Ignatova et al. 2007). Finally, it has shown that also some purification tag, such as the glutathione S-transferase fusion does affect the aggregation dynamics of polyQ (Perutz 1994).

interactions within an amphipathic α-helical structure of N17 (Thakur et al. 2009). Accordingly, the deletion of this region strongly reduces polyQ aggregation *in vitro* (Thakur et al. 2009). These results suggest that the regions outside the polyQ tract may interact with each other, influencing aggregation (Truant et al. 2008; Zuccato et al. 2010).

The ***first*** proposed polyQ aggregation pathway was mediated only by aggregation of the polyQ stretches (Bates 2003; Ross & Poirier 2004; Wanker 2000). It displayed the kinetics of nucleated-growth polymerization with a prolonged lag-phase required to form an aggregation nucleus, followed by a fast extension phase during which additional polyQ monomers rapidly joined the growing aggregate.

The ***second,*** recently proposed, aggregation pathway comes from Wetzel's group (Kar et al. 2011; Thakur et al. 2009). This depends mainly on N17 and involves several intermediates. In particular, the aggregation process may be characterized by the formation of oligomers having N17 in their core and polyQ sequences exposed on the surface. As the polyQ length increases, the structure decompacts and oligomers or protofibrils rearrange into amyloid-like structures capable of rapidly propagating via monomer addition (Kar et al. 2011; Thakur et al. 2009). The importance of the flanking regions suggests other therapeutic targets for polyQ-mediated neurodegeneration related to N17 or polyP, rather than polyQ itself.

2. Computational studies of Huntington Disease

In the following paragraph we provide an overview of the computational studies present in the literature carried out on the different aspects of HD such as the structure of the oligomers, the factors driving the formation and determining the thermodynamic stability of amyloidogenic aggregates and the role of the flanking regions on aggregation mechanism. All these studies are grouped on the basis of the topic and of the computational methods employed to address them.

2.1 Structural models of polyQ oligomers — Atomistic simulations

Many aspects of the HD's onset mechanism could be elucidated obtaining structural information at atomistic level on polyQ aggregates. However, detailed structural information are difficult to obtain experimentally as short wild-type polyQ tracts are insoluble at the high concentrations required for crystallographic or NMR studies (Truant et al. 2008).[f] In contrast, structural information at atomic level of resolution can be provided by computational approaches (Moroni et al. 2009; Miller et al. 2010). Simulations, in fact, can offer insights into structural and dynamical properties of polyQ peptides of different lengths, shapes and oligomeric states. Computational studies of neurodegenerative diseases can be carried out via classical molecular dynamics (MD) (Miller et al. 2010; Ma & Nussinov 2006). In this method, the atoms move according to the Newton's law on a predefined

[f]A simple search within the PDB (http://www.rcsb.org/) reveals that polyQ tracts present in a variety of normal cellular proteins are annotated as 'unstructured' or have to be removed to facilitate crystallization (Truant et al. 2008). Only one structure exists of the N-terminal part of Htt with 17Qs, obtained by a fusion with maltose-binding protein. It features polyQ stretch that can adopt an α-helical, random-coil, or an extended-loop conformation (Kim et al. 2009).

potential energy surface. Namely, interatomic interactions are described via empirical force fields. However, MD simulations in explicit water allow accessing a time scale limited to hundreds of ns. Thus, to simulate relevant biological processes, occurring on longer time scales, they have to be combined with enhanced sampling computational techniques (Christ et al 2010; Laio & Gervasio 2008) or it is, otherwise, necessary to use simplified interaction potentials (Ma & Nussinov 2006; Tozzini 2010; Miller et al. 2010).

Several structural models of the aggregated polyQ units were proposed with geometries compatible with available experimental information (electron microscopy and X-ray data). These models were based on Perutz's suggestion that Q side chains, being similar to the amino acid backbone units, could establish an H-bond network (Perutz 1999; Perutz 1994). In fact, Perutz, initially interpreted the X-ray diffraction data of polyQ aggregates as a polar zipper model, and later reinterpreted them as a circular β-helix model in which polyQ tracts can form turns composed by 20 res, with the Q side chains alternatively inside and outside the water filled nanotube (Fig. 2). According to this model, polyQ aggregates would be stabilized by H-bond interactions between main and side chain atoms (Fig. 2). In fact, the β-sheets were proposed to be antiparallel so that an amine group of one side chain could H-bond with the carbonyl group of the side chain belonging to the following turn (Esposito et al. 2008). Consistent with these X-ray diffraction data is also triangular β-helix model (Stork et al. 2005; Raetz & Roderick 1995), which is formed by turns of 16 residues, and the Atkins's model, in which the H-bond network of the Q side chains allows for high-density packing (Sikorski & Atkins 2005). Although several models were proposed for the polyQ aggregates, this issue is highly debated and it is still not clear which is the most common structure present in the aggregates.

Many studies of the proposed models for the polyQ aggregates were preformed via classical MD simulations (Perutz 1994; Perutz et al. 2002; Sikorski & Atkins 2005; Sunde & Blake 1997; Sunde et al. 1997; Sharma et al. 2005), providing valuable insights on their stabilities (Sikorski & Atkins 2005; Esposito et al. 2008; Stork et al. 2005; Armen et al. 2005; Finke et al. 2004; Finke & Onuchic 2004; Marchut & Hall 2006, 2006, 2007; Merlino et al. 2006; Zanuy et al. 2006; Ogawa et al. 2008). Among these, several studies investigated the dependence of the structural stability of the circular β-helix, as well as of other possible structures, on the Q length (Stork et al. 2005; Merlino et al. 2006; Ogawa et al. 2008; Rossetti et al. 2008; Hajime et al. 2008; Khare et al. 2005), leading sometimes to conflicting views. For example classical MD studies showed that β-helices with three turns were unstable with circular geometries, being, instead, stable in a triangular β-helix shape. Moreover, these studies pointed out that two-coiled triangular polyQ β-helices, which were individually unstable, became, instead, stable upon dimerization. This suggested that the formation of the initial aggregation seed of huntingtin amyloids requires dimers of at least 36 Qs (Stork et al. 2005). A subsequent study verified the stability of the circular β-helix model by performing MD simulations on polyQ fragments of different lengths. The results pointed out that circular β-helix models maintained a regular structure during the MD run, only when containing more than 40 Qs (Merlino et al. 2006). Moreover, a different MD study showed that the stability of the circular β-helix structure increased with an increasing number of Q, reaching the maximal stability above 30 Qs (Ogawa et al. 2008). In contrast to these computational results, annular units smaller than the circular β-helix model were detected experimentally and confirmed by other computational studies

(Marchut & Hall 2006a, 2006b, 2007; Papaleo & Invernizzi 2011). A more recent MD study proposed a systematic investigation of structural characteristic of polyQ strands in the early stage of nucleation, considering left handed circular, right handed rectangular, left and right handed triangular β-helices of different lengths (Zhou et al. 2011). These simulations showed that left handed triangular and right handed rectangular conformations were stable when they had at least three turns, preserving a high degree of the β-sheet content during the simulation. The stability of the systems increased with an increasing number of rungs, but it was insensitive to the number of Qs in each polyQ fragment (Zhou et al. 2011). Classical MD simulations were also performed for the cross-β-spine steric zipper model (Esposito et al. 2008), a motif found for the GNNQQNY peptide, an heptapetide present in the N-terminal prion-determining domain of the yeast protein Sup35. The simulations revealed that this kind of polyQ assemblies were very stable. In fact, the H-bonds between either parallel or antiparallel β-sheets, greatly affected the high stability of these structures, with a large contribution coming from the Q side chains H-bonds.

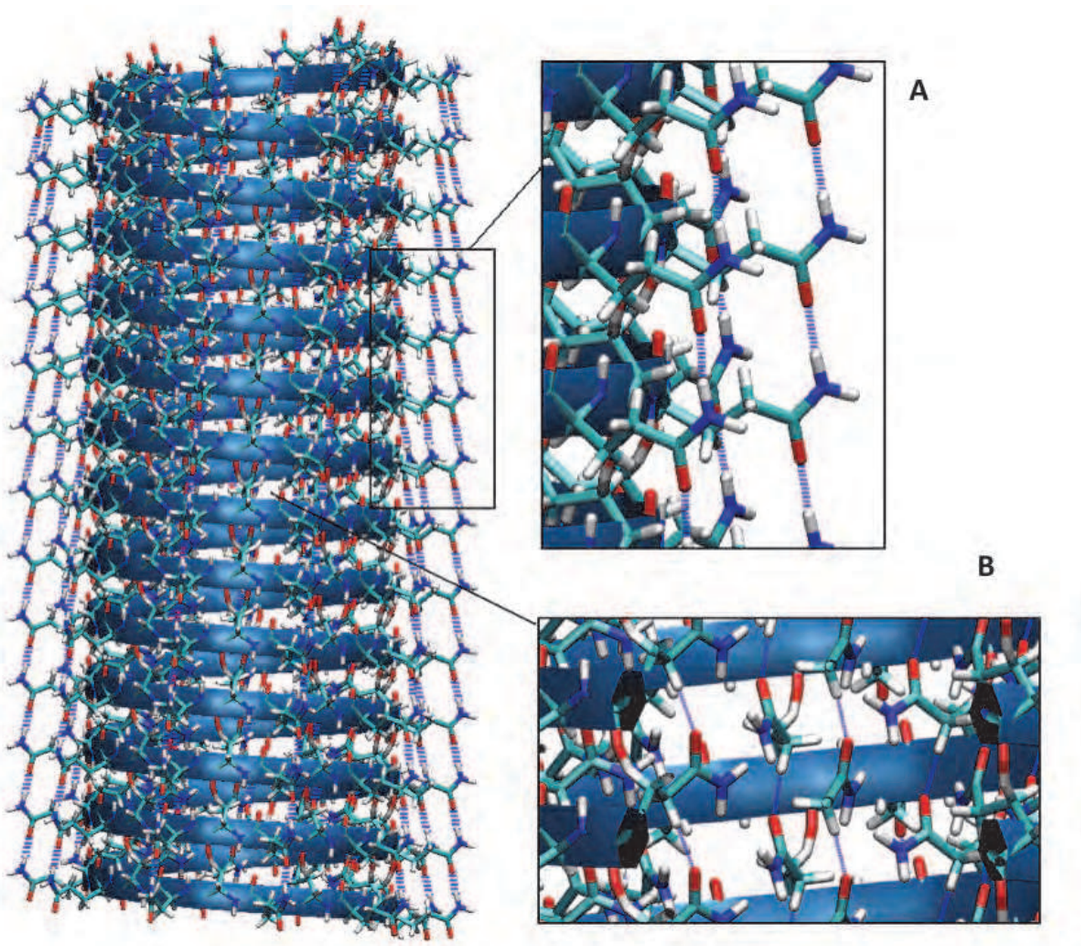

Fig. 2. Molecular view of circular β-helix structure with particular of: A) external and B) internal H-bond network. A similar H-bond network is observed also for the triangular β-helix structure.

In summary, all these computational studies suggested that several polymorphic forms of polyQ oligomers can exist and that all of them, when present as monomers, become more stable with an increasing number of Qs or upon aggregation with other polyQ tracts. The polymorphism of polyQ structures may possibly result in different pathways leading to the formation of toxic oligomers and fibrils.

2.2 Cooperativity of polyQ H-bonds — *ab inito* and Hybrid QM/MM simulations

Computer simulations can also help in elucidating the role of the peculiar electronic properties of the Q side chains in the formation of polyQ the aggregates. β-sheets are ubiquitous in protein structures and in aggregates of amyloidogenic proteins (Tartari et al. 2008). Thus, understanding the electronic factors contributing to the thermodynamic stability of β-sheets is of fundamental importance in neurodegeneration (Rossetti et al. 2010). In the past, several research groups tried to address experimentally and computationally whether the formation of β-sheets is cooperative. Cooperativity in H-bonding exists from a structural and from an energetic point of view when the strength of H-bonds and the thermodynamic stability of the H-bonding structures, respectively, increase non-linearly with an increasing number of H-bonds. From an electronic point of view H-bond cooperativity depends on the polarization of the electronic clouds of adjacent molecules or strands. If, polarization effects are present, a rearrangement of electronic structure takes place. This aspect is clearly not accounted in force field calculations, which are grounded on predefined parameters of the potential energy. Thus, despite the successes of classical MD simulations in the study of neurodegenerative diseases, there are cases in which the use of effective potentials may be not accurate enough. In these cases a more sophisticated computational approach is provided by static or dynamics *ab initio* calculations, typically based on Density Functional Theory (DFT). In static DFT calculations the electronic structure problem is solved parametrically for nuclear configurations generated by minimization schemes. Instead, in dynamic DFT calculations the atoms move according to the Newton's law on a potential energy surface, which is evaluated from electronic structure calculations (Spiegel & Magistrato 2006; Carloni et al. 2002). Clearly, *ab initio* schemes, requiring to solve the electronic structure problem for different nuclear configurations, are much more computationally demanding than classical MD, limiting the size of the systems studied to hundreds of atoms and the time scale accessible to *ab initio* MD to tens of ps (Carloni et al. 2002). Since biological systems treated in their environment comprise several hundreds of thousands of atoms, they are clearly too large to be treated with a full *ab initio* description. An alternative approach to treat these systems relies on hybrid quantum-classical (QM/MM) MD simulations. The QM/MM MD approach combines classical with *ab initio* MD. In this approach the system under investigation is divided into two different regions, allowing to concentrate the computational efforts of the electronic structure calculations (QM part) to the part in which the force field can fail. The rest of the system is, instead, treated with empirical force fields in a computationally more efficient manner (Spiegel & Magistrato 2006). This allows to extend the size of the systems studied to hundreds of thousands of atoms, although the computational cost of the QM part still limits the time scale accessible to few tens of ps.

The role of cooperative effect (CE) of H-bonds between different strands of amyloidogenic aggregates was investigated by performing static DFT calculations on the known molecular

structure of the heptameric peptide GNNQQNY. This study showed that the strength of H-bonds between layers of fibrils increased nonlinearly up to four layers. Moreover, it showed that the H-bonding interactions within the β-sheets of the amyloid structure were cooperative, with contributions to the binding energy from several layers away within the fibril (Tsemekhman et al. 2007). Other studies carried out on polyAlanine (A), polySerine, polyValine homo-polymers showed that H-bonding and dipole–dipole interactions were strengthened through CEs, contributing to the stability of the secondary structures (Horvath et al. 2004, 2005; Varga & Kovács 2005; Improta & Barone 2004; Improta et al. 2001; Improta et al. 2001; Wieczorek & Dannenberg 2003). In these studies the influence of the side chains on the thermodynamic stability of the investigated structures was also verified. These results highlighted the presence of cooperativity in the C=O..H-N H-bond, which was an important source of long-range interactions (Horvath et al. 2005). Instead, DFT calculations performed on polyGlycine (G) of different lengths and conformations showed the influence of long-range effects on the stability of different conformers (Improta & Barone 2004; Improta et al. 2001; Improta et al. 2001). Moreover, long-range interactions were shown to contribute considerably to the stability of the β-sheet structures, with appreciable effects on the molecular geometry. It was also shown that the H-bond length was very sensitive to long-range interactions (Horvath et al. 2004, 2005). Finally, a DFT study carried out also on polyG peptides showed that repeating H-bonds either in parallel and antiparallel β-sheets were not cooperative in terms of enthalpy contribution in the direction parallel to strand elongation. CEs existed, instead, in the perpendicular direction and they depended on the number of residues in each strand (Zhao & Wu 2002). Thus, all these studies suggested that H-bond CEs exist in homopolypeptides in different conformations, including the β-sheet structure. Since the Q side chain resembles an animoacid backbone, it is likely that CEs will greatly contribute to H-bond cooperativity and to the thermodynamic stabilization of the polyQ β-sheets. This aspect was addressed recently by performing *ab initio* and QM/MM MD calculations (Rossetti et al. 2010).

2.3 Aggregation properties and the role of exon-1- coarse grain models and enhanced sampling techniques

The details of molecular mechanism leading from the association of monomeric polyQs to the formation of mature fibrils remain highly debated. As mentioned above, Wetzel at al. suggested initially a nucleated grow polymerization model based only on the polyQ peptides to connect the disordered monomers to the highly ordered β-sheet structures present in the fibrils (Papaleo & Invernizzi 2011).

Several computational studies were carried out to shed light on the aggregation properties of polyQ chains, on the formation of the initial aggregation nucleus and on the role of the regions flanking the polyQ tract in m-Ex1 (Papaleo & Invernizzi 2011). A common methodology employed in these studies was the use of coarse grain (CG) models, in which groups of atoms are described as a single bead (Tozzini 2010). In the simplest model only three types of beads, namely hydrophobic, hydrophilic and neutral, are considered. Other CG models instead have special terms to account for H-bond formation, which is crucial for aggregation (Ma & Nussinov 2006). CG methods usually allow to extend the time scale accessible to MD simulations, loosing, at the same time, the accuracy of an atomistic description. Sometimes atomistic simulations with the use of implicit solvent models give an

alternative to the CG models. However, an explicit treatment of the solvent is of crucial importance for a correct characterization of the folding and of the aggregation properties of polypeptides (Papaleo & Invernizzi 2011). Conversely, atomistic simulations can be used in combination with methods, which allow to extend the time scale of the simulations, enhancing the sampling of the underlying free energy surface (Laio & Gervasio 2008; Christ et al. 2010; Biarnes et al. 2011; Sugita & Okamoto 2000; Bussi et al. 2006). These latter warrant the accuracy of the atomistic description, but they are computationally very demanding and, in most cases, not yet at the stage of being able to simulate the folding and/or the aggregation of peptides of the biologically relevant lengths (Rohrig et al. 2006; Miller et al. 2010). Among the aggregation studies carried out so far for HD, a force filed based monte carlo simulation study in implicit solvent (Vitalis et al. 2009) investigated the free energy cost associated with the formation of ordered β-sheet structures in dependence an increasing number of Qs in the single monomer (Vitalis et al. 2009). This work reported the free energy costs to form structures with a high β-sheet content consistent with literature data. However, an increase of this free energy cost with an increasing chain length was observed, in contrast to previous interpretation of kinetic data. Moreover, the authors suggested that β-sheet formation may be an attribute of peptide-rich phases characterized by high molecular weight aggregates rather than monomers or oligomers (Vitalis et al. 2009).

Discrete Molecular Dynamics (DMD), an efficient MD method based on a simplified interparticle potential (Miller et al. 2010), was employed to show that the cooperativity in the folding of a chimeric monomer (composed by Chymotrypsin inhibitor 2 with an inserted polyQ repeat) decreased for peptides with polyQ lengths above the pathogenic threshold. Moreover, it was demonstrated that the dominant mode for dimer formation was inter Qs H-bonding (Barton et al. 2007). The aggregation of model polyQ peptides was also investigated via MD simulations with a simplified model of polyQ (Marchut & Hall 2006a, 2006b, 2007). This model accounted for the most important types of intra- and inter-molecular interactions, namely H-bond and hydrophobic interactions, allowing the folding process to take place within the time scale of the simulation (Marchut & Hall 2007). In this study the folding of isolated polyQ tracts of non-pathogenic and pathogenic lengths, and the folding and the aggregation of systems of polyQ peptides of various lengths were investigated. The isolated polyQ peptides formed some backbone–backbone H-bonds, although the hydrogen bond content (HBC) was markedly lower than that of an ordered β-sheet structure. In the multi-chains simulations, instead, ordered aggregates with significant β-sheet and random coil characters were observed at intermediate and high temperatures, respectively. Interestingly, the temperature at which the peptides underwent the transition from amorphous to ordered aggregates and from ordered aggregates to random coils increased with increasing polyQ length. More recently, the aggregation of polyQ peptides of different lengths was addressed via replica exchange (RE) MD and a simplified force filed. REMD simulations combine several MD simulations at elevated temperature to generate a variety of conformational ensembles with a Monte Carlo like conformational selection (Bussi et al. 2006). Thus, this method allows to explore the conformational space of peptide aggregation and folding, instead of getting trapped in local minima (Sugita & Okamoto 2000). In this work REMD was applied to study the aggregation kinetics of the polyQ monomers and dimers with chain lengths from 30 to 50 residues. The results showed that for the monomers a structural change from an α-helical structure to random coil occurs with no formation of a β-strand. For dimers, instead, starting from random coils there was the

initial formation of antiparallel β-sheets, of circular and of triangular β-helices, which may lead to the formation of toxic oligomers and fibrils (Laghaei & Mousseau 2010).

As stated previously, the sequences flanking the polyQ tract have been recently demonstrated to have a key role on aggregation mechanism (Thakur et al. 2009). However, structural information on these segments are lacking. Thus, more recent computational studies employed the classical MD method in combination with enhanced sampling techniques to investigate the complex free energy landscape for the folding and for the aggregation of the N terminal region of Htt (Ex1 or N17). These studies are of crucial importance to understand how the misfolding and aggregation of polyQ tract(s) is affected by the flanking sequences.

Classical MD studies in combination with simulated tempering and folding at home infrastructure were employed to study the thermodynamics of N17 (Kelley et al. 2009). In these simulations N17 was found to be highly helical, although adopting two different and seemingly stable states. The most populated state was a two-helix bundle, although a significant percentage of structures still assumed the conformation of a single straight helix. Since N17 was demonstrated to be involved in the rate-limiting step for the formation of the initial aggregation nucleus, two possible mechanisms for the nucleating event were proposed in this study. These are based on a transition between the two-helix and single-helix state of N17 and on the interactions between the N17 and the polyQ tract (Kelley et al. 2009). Moreover, a recent Monte Carlo simulation study, along with circular dichroism experiments, described the effect of N17 on polyQ conformations and intermolecular interactions. This study showed that N17 and polyQ domains were increasingly disordered as the polyQ length increased in N17-polyQs peptides. In contrast with experimental suggestions (Thakur et al. 2009), N17 suppressed the intrinsic propensity of the polyQ tracts to aggregate by forming incipient micellar structures adopted by N17 segments. Instead, increasing the polyQ length the degree of intermolecular association increased, becoming mainly governed by the associations between polyQ tracts (Williamson et al. 2010). Finally, a systematic DMD study, in combination with the RE method, was carried out on monomeric Ex1 with the full flanking regions on a variant of Ex1 missing the polyP region, which is hypothesized to prevent aggregation, and on an isolated polyQ peptide. For each of these three constructs, polyQ tracts of pathogenic and non-pathogenic lengths were considered. Interestingly, the study showed a correlation between the length polyQ tract and the probability to form a misfolded state rich in β-sheets. Furthermore, it showed that N17 more likely adopted a β-sheet rather than an α-helix conformation as the length of the polyQ tract increased. Finally, this study demonstrated that the polyP region formed polyP type II helices, decreasing the probability of the polyQ to form a state rich in β-sheets (Lakhani et al. 2010). More recently, enhanced sampling techniques were employed to predict the conformational properties of N17 fragments in water solution and to shed light on its crucial role in Htt aggregation (Kar et al. 2011).

3. Selected applications

In the following paragraph we present three selected examples taken from our work in which we explain in detail how computer simulations can be employed to address the different, still unclear, aspects of the HD's onset mechanism.

3.1 The HD threshold and the structural stability of toxic conformers

In this work we have addressed one of the questions lengthily debated concerning the polyQ length-dependent toxicity threshold. One hypothesis suggested that the length dependent toxicity of HD was based on a specific structural transition, occurring only when the polyQ tract is above 36 amino acids (structural transition hypothesis). Consistent with this hypothesis, an anti-polyQ monoclonal antibody was observed, which was able to specifically recognize the expanded toxic polyQ tracts. This suggested the existence of a generic conformational epitope formed only above a certain polyQ length (Trottier et al. 1995; Kaltenbach et al. 2007; Sugaya et al. 2007). The presence of such abnormally folded protein, which can aggregate and form fibrillar structures, could highlight similarities between HD and other neurodegenerative diseases such as Alzheimer's, Parkinson's D, and prion disorders (Ross & Poirier 2004). Hence, several efforts were done for "hunting the elusive toxic polyQ conformer" (Trottier et al. 1995). This hypothesis was, however, challenged by various experimental evidences. First, polyQ fragments shorter than the disease threshold were also shown to aggregate, adopting similar structures to those of peptides longer than threshold (Klein et al. 2007; Masino et al. 2002; Bennett et al. 2002; Tanaka et al. 2001) and to exhibit toxicity in an eukaryote organism (*Caenorhabditis elegans)* (Morley et al. 2002). Second, it was shown that polyQ length influences the stability of the initial aggregation seed and that, in turn, it may affect the kinetics of its formation (Chen et al. 2002). The kinetics of the elongation phase is, instead, independent of the polyQ length (Chen et al. 2002). Furthermore, it was suggested that the toxicity of mut-Htt may be simply due to the fact that polyQ tracts are inherently toxic sequences, whose deleterious effects gradually increase with their length (Klein et al. 2007). We investigated the influence of the polyQ length on the structural stability of monomers and oligomers by performing atomistic MD simulations on different β-helical models featuring a number of Qs below and well beyond the disease threshold (Rossetti et al. 2008). We considered the circular (Raetz & Roderick 1995) and triangular β-helices (Stork et al. 2005; Perutz et al. 2002) as shapes of the oligomers, since these are the only models consistent with the 'structural threshold hypothesis'. Thus, we studied two large monomeric models based on the circular β-helix (labeled as P from Perutz, who introduced this model in 2002 (Perutz et al. 2002)), and on the triangular β-helix model (labeled as T). This latter was constructed starting from the regularly shaped coils of UDP-N-acetyl glucosamine acyltransferase (Raetz & Roderick 1995) (Protein Data Bank entry: 1LXA) (Berman 2000), and replacing each residue with a glutamine. The circular and triangular β-helix models contained 266 and 179 residues and each turn was composed by 20 and 18 Qs, respectively. Both the T and the P models were composed by a single polyQ chain and had a number of Qs well above that observed at physiological conditions. In addition, we considered different oligomeric models built starting from the single chain P and T systems: (i) 4 oligomers in circular β-helix conformation composed by 4, 3, 2, 1 monomers (each composed by 40 Qs). These were named P_{AD}, P_{AC}, P_{AB}, P_A, respectively. (ii) 4 oligomers in triangular β-helix conformation with respectively 4, 3, 2, 1 monomers (each composed by 36 Qs). These models were symbolized by T_{AD}, T_{AC}, T_{AB}, T_A , respectively. (iii) One oligomer in circular β-helix conformation composed by 8 monomers each containing 25 Qs residues. The model was named $P_{AH25.}$ (iv) Finally, we considered 4 small monomeric models in circular β-helix conformation composed by 25, 30, 35, 40 Qs and symbolized by P_{25}, P_{30}, P_{35}, P_{40}, respectively.

These models were chosen to perform a systematic study that allowed us to validate or discard the 'structural threshold hypothesis'. Moreover, by varying systematically the size of the polyQ units in these models, and considering both the monomeric and oligomeric states, our calculations shed light on the dependence of the stability of β-helical structures upon the number of monomers. Finally, considering both the P and T helical structures, our findings became independent of the structural model chosen. To simplify the discussion we defined qualitatively the Structural Stability (SS) as a quantity which increased (i) with the compactness of the structure, as measured by the plots of the RMSD of backbone atoms, as well as the gyration radius (*R*g) versus time and (ii) with the HBC, defined as the total number of H-bonds formed within the structural models, divided by the total number of H-bond donor functionalities. Our MD simulations at finite temperature and in aqueous solution pointed out that the two different β-helix shapes influenced only the β-sheet content. In particular, the T helix displayed a larger number of residues in random coil conformation than the P one. However, the HBC as well as the SS of the two shapes were comparable (Fig. 3). Moreover, we demonstrated that SS did not depend on the number of Qs in the monomers. In fact, oligomers composed by 4 monomers of 40 Qs and by 8 monomers of 25 Qs had similar SS. Consistent with our results an NMR study revealed no structural difference between aggregates formed by short and long polyQ peptides (Klein et al. 2007). We also showed for the first time that the SS of polyQ oligomers was not affected by the shape. We suggested, instead, that only the number of monomers – thus, the concentration in an (*in vivo* or *in vitro*) experiment - contributes to the overall stability of the oligomers. This may be due to the additive contribution of the single monomer in the H-bond network formed between backbone atoms (Fig. 3).

Conversely, the H-bonds formed between Q side-chains influenced mainly the stability of the single isolated monomers (Fig. 4). In fact, the isolated monomer with Q length above the disease threshold, P_{40}, was characterized by a larger number of β-sheet content and HBC, with respect to shorter monomers (Fig. 4). This latter depended mainly on side chain H-bonds, and thus, on the number of Qs. Therefore, if the Q length was lower than that of the disease threshold, the β-stranded monomers were unstable and, hence, they might aggregate with lower probability (Fig. 4), consistent with experimental findings.

In conclusion, our data discarded the structural threshold hypothesis. However, interpreting our findings on the basis of the whole landscape of available experimental data (Klein et al. 2007), we suggested that the observed length-dependent toxicity threshold may be explained by a faster aggregation kinetics, occurring for longer polyQ tracts.

3.2 Hydrogen bonding cooperativity in polyQ β-sheet investigated by *ab initio* and QM/MM MD simulations

Perutz was the first to show that the polyQ tracts may form β-sheet based structures, which are able to establish tighter interactions with increasing polyQ length. Therefore, the correlation between the strength of the polyQ chain and the strength of the interactions may be a key aspect at the basis of the correlation between polyQ length and severity of disease (Perutz 1994). Peruz suggested that this may be due to the Q side chain, which, having the same chemical characteristics of an amino acid backbone, can form a network of H-bonds involving both the main and the side chain atoms (Perutz 1994; Klein et al. 2007; Perutz &

Windle 2001)[g]. CE in H-bonding is very important for both the structure and the energetic of polypeptide systems. As the presence of CE was demonstrated for other homopolymers, it is likely that this effect may be particularly relevant in the peculiar H-bond network of polyQ, playing a key role in Htt/Ex1 misfolding and aggregation (Perutz 1994; Perutz & Windle 2001). Most of the studies carried out on the structural stability of polyQ oligomers

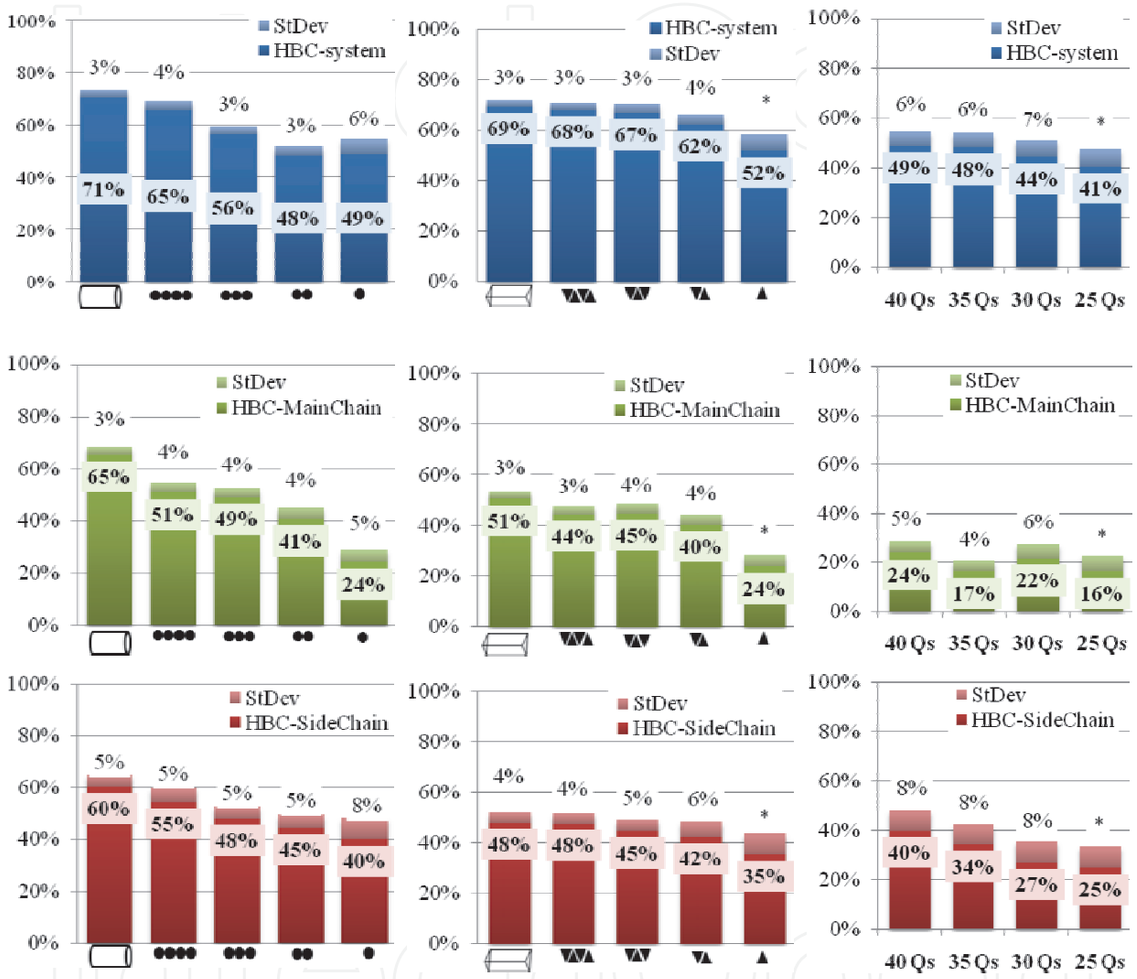

Fig. 3. HBC in P and T series given as percentage of H-bonds in the P series (left column), in the T series (middle column) and in the monomeric series (right column). Blue, green and red histograms represent the total, the main chain and the side chain HBC, respectively. The solid cylinder refers to the P model and the black circles refer to monomers of 40 Qs in circular β-helix. The triangular cylinder refers to the T models and the black triangles refer to monomers of 36Qs in triangular β-helix shape. Monomers of different lengths are indicated with the number of Qs present in the chain.

[g]Consistently with this hypothesis, aggregates of protein are not seen in proteins expressing polyasparagine, an amino acid that differs from glutamine even by only one methyl group (Oma et al. 2004).

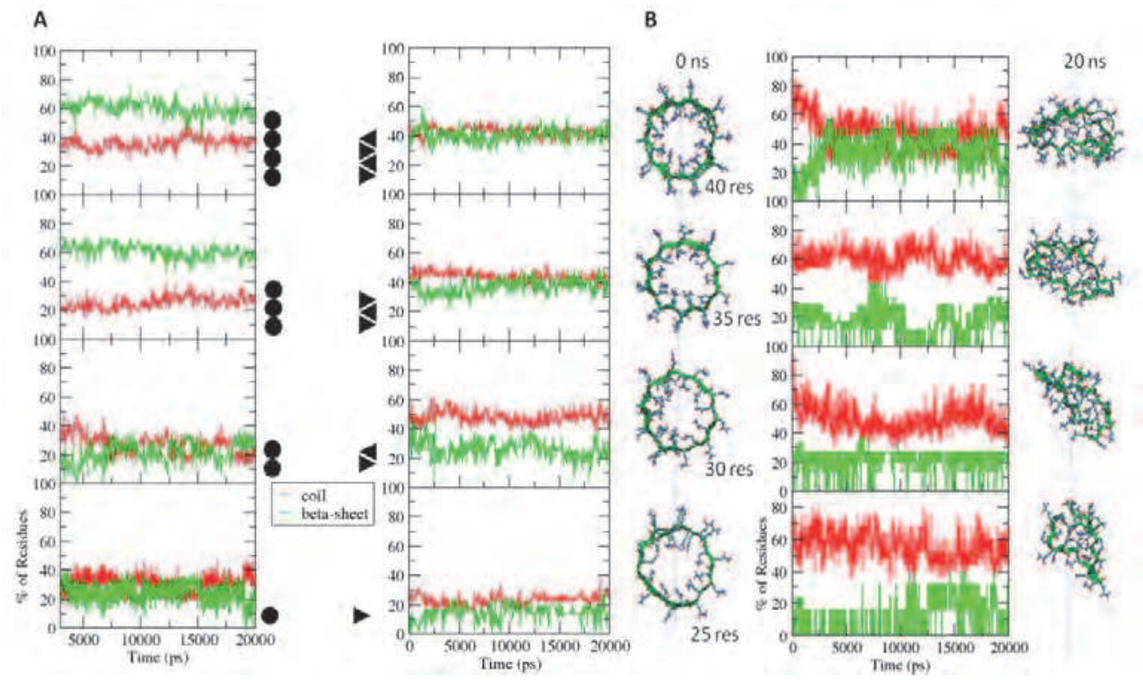

Fig. 4. β-sheet (green) and random coil conformation (red) of oligomers in circular (left panel) and triangular (middle panel) β-helix conformations, symbolized as black circles and triangles, respectively (A) and of P_{40}, P_{35}, P_{30}, P_{25} monomers (B) (right panel). Monomers of different lengths are indicated with the number of Qs present in the chain. On the left and right side of the graph in B the initial and final (after 20 nanoseconds (ns) MD) geometries of each monomer are shown. Water is not shown for clarity.

were achieved by classical MD calculations, which, not dealing with electronic polarizability, were not suitable to characterize the presence of CE in this kind of aggregates. CE was investigated on other polypeptides (Tsemekhman et al. 2007; Varga & Kovács 2005; Horvath et al. 2004, 2005; Improta & Barone 2004; Improta et al. 2001; Improta et al. 2001; Zhao & Wu 2002; Wieczorek & Dannenberg 2003; Viswanathan et al. 2004; Scheiner & Kar 2005) with the application of first principle methods. However, here we provide a summary of the first study in which the presence and the importance of CE in the H-bonds of Qs side chains was verified with DFT approaches (Rossetti et al. 2008). We performed first principles DFT-PBE (Benedek et al. 2005; Morozov et al. 2004; Perdew et al 1996) calculations on polyQ peptides of increasing complexity, assembled in parallel[h] β-sheets (Tsemekhman et al. 2007; Koch et al. 2005; Beke et al. 2006; Perczel et al. 2005). In order to carry out this study we used different models[i] (labeled as *N*x*n* hereafter), which differed from each other for the number of strands (*N*=1, 2, 3, 4) and/or for the number of Qs in each strand (*n*=1, 2, 3, 4).[i] The resulting 16 models ranged from 29 to 320 atoms. Furthermore, to verify the contribution of the polyQ side chains to CE we also considered a series of models where we varied the initial Q side chains conformations putting them in a position in which they could not H-

[h]CE turns out to be stronger in parallel β-sheets (like the systems considered here) than in anti-parallel ones (Koch et al. 2005).
[i]The models were built using HyperChem 8.0 program (Hypercube)
[i]Each polypeptide is terminated by the addition of -NCH3 and -OCCH3 groups.

bond with the adjacent strand and, a series of models built with polyA. Finally, to check the role of solvent and temperature effects on polypeptide conformation (Scheiner & Kar 2005) we performed 2 *ps* of hybrid DFT/MM MD calculations on a large a β-helix nanotube (8 turns of 20 Qs) in aqueous solution (Perutz et al. 2002; Berendsen et al. 1995; CPMD; 2002; van der Spoel et al. 2005). In this case, we considered three models in which the QM part included the *4x4*, *3x4* and *4x3* moieties.

Although circular β-helix is only one of the possible polyQ structures (Sikorski & Atkins 2005; Zanuy et al. 2006), we investigated it since we demonstrated by classical MD studies that the structural stability of the polyQ oligomers was independent from the β-sheet shape (Rossetti et al. 2008). In this study, in fact, we aimed at providing a qualitative description of CE. Quantitative predictions would, instead, require an investigation on a variety of proposed structures. CE on β-sheet strands may be present in patterns *perpendicular* to the peptide elongation (⊥ CE) or *parallel* to it (||CE) (Fig. 5A). When ⊥ CE is present a decrease in H-bond length should be observed with an increasing number of strands. Moreover, in ∞CE the H-bonds at the center of the pile should be shorter than at the rim. Consistent with the presence of ⊥ CE, in all models considered the H-bond distances of both the backbone and the side chains decreased with an increasing number of strands. In addition, H-bond lengths turned out to be shorter at the center of H-bonded chains than at the rim when at least three H-bonds were piled up in the perpendicular direction (***N***= 4). This feature was observed both for the side chains and the backbone. Interestingly, it was observed that the backbone dipoles along the same column (H-bond in the perpendicular direction) of β-strands had the same orientations (in contrast to those of the adjacent column) and could, therefore, sum up increasing the polarization of the systems (Zhao & Wu 2002). However, in the peculiar case of polyQ β-strands, the Q side chains counterbalanced this polarization, affecting the H-bonds of the backbone. As a result, in the columns where the H-bond dipole orientations were enhanced by similar side chain H-bond dipole orientations, a ⊥ CE was present. This resulted in a H-bond shorter at the center of the column. On the other hand, when neighboring side chain columns had H-bond dipoles oriented in opposite directions (with respect to the column considered), the inner H-bond was not the shortest of the column (Fig. 5 D and E). This explains why for the backbone the ⊥ CE, namely the fact that H-bonds are shorter at the center of the pile and not at the rim, was visible only by tacking averages (Fig 5D).

A different type of CE is that parallel to peptide elongation (||CE). When ||CE is present, a shortening of the central H-bond lengths between two adjacent strands takes place. This is usually not present in β-sheets due to the alternative orientation of backbone H-bond dipoles along the strands. However, the dipoles associated with the Q side chains added up in a coherent way for the central H-bonds between two strands (Fig. 5E). This occurred at position 2 in ***N*** × 2 series, at positions 2 and 3 in ***N***× 3 series and at positions 2, 3, and 4 in ***N*** × 4 series. Thus, these H-bonds were shorter than those of the rim. As expected, in the calculations in which the side chains were impaired of H-bonding or Qs were replaced by As, the ||CE was not observed. QM/MM MD calculations qualitatively reproduced the H-bonds trends of the corresponding *in vacuo* models. However, in these simulations H-bond lengths were larger and the side chains formed mostly H-bonds with the solvent. These differences were probably due to the presence of the solvent and to temperature effects, which were completely neglected in the *in vacuo* calculations. These calculations suggested that environmental effects influence only the magnitude of CE in H-bonding, while the qualitative trend was the same of that found in the *in vacuo* calculations.

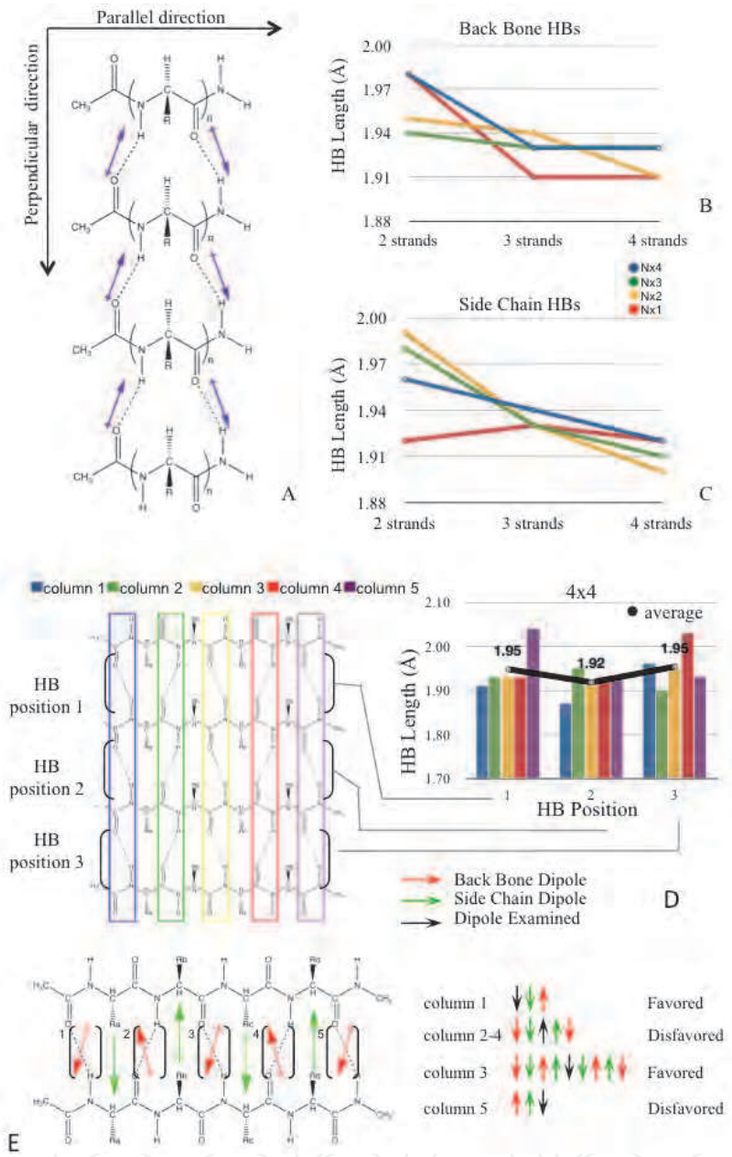

Fig. 5. Cooperative Effect - A) Definition of CE in H-bonds parallel (||) and perpendicular (⊥) directions to peptides elongation. B)-C) Structural aspects of CE: B) Backbone CE (⊥CE): Mean values of H-bond lengths of the backbone atoms versus the number of strands for each series of n Qs. C) Side chains CE (⊥CE): Mean values of H-bond lengths for the side chain atoms versus the number of strands for each series of n Q. D)-E) ⊥CE in system 4x4. D) In the histograms: H-bond length of backbone for different positions inside each strand as a function of the position across the different strands. Color of the histogram corresponds to the H-bonds circled on the left picture of B. The black line connects the mean values over the rows. E) Orientation of dipoles associated with the H-bonds for the 4x4 system. Consistent with these results, in the simulations in which the Q side chains were impaired to H-bond and in the models in which the Qs were replaced by As, the H-bond at the center of the polyQ chain was longer than at the rim. The H-bond lengths, instead, continued to decrease with the number of piled strands even in these systems.

Finally, we also calculated the stabilization energy associated with the formation of H-bonds between the different strands of the systems *in vacuo.* To this end we defined the stabilization energy *per strand* (ΔE_N) as the energy associated with the addition of the N^{th} Q strand to the Q_{N-1} strands ($E_{N\times n}$), minus the formation energy of the N isolated strand ($\Delta E_N = E_{N\times n} - N \cdot E_{1\times n}$). In this definition, $E_{N\times n}$ is the energy of a system containing N strands and belonging to the n series; while $E_{1\times n}$ is the energy associated with an isolated strand containing n Qs. In practice this is the energy of a strand containing n Qs isolated from long-range effects. We also introduced the stabilization energy per H-bond (ΔE_{HB}) as Δ_{EN} divided by the number of H-bonds (n_{HB}) in each system ($\Delta E_{HB} = \Delta E_N / n_{HB}$).

Our study showed that ΔE_{HB} decreased nonlinearly with the number of strands (Fig. 6). ΔE_{HB} ranged from -5.0 kcal/mol in the smallest system to -6.5 kcal/mol in the larger system, suggesting that a CE existed and that for the present systems this was at most of 1.5 kcal/mol per H-bond. Clearly this stabilization energy was smaller for models containing A residues and with Qs side chains rotated to impair H-bonding.

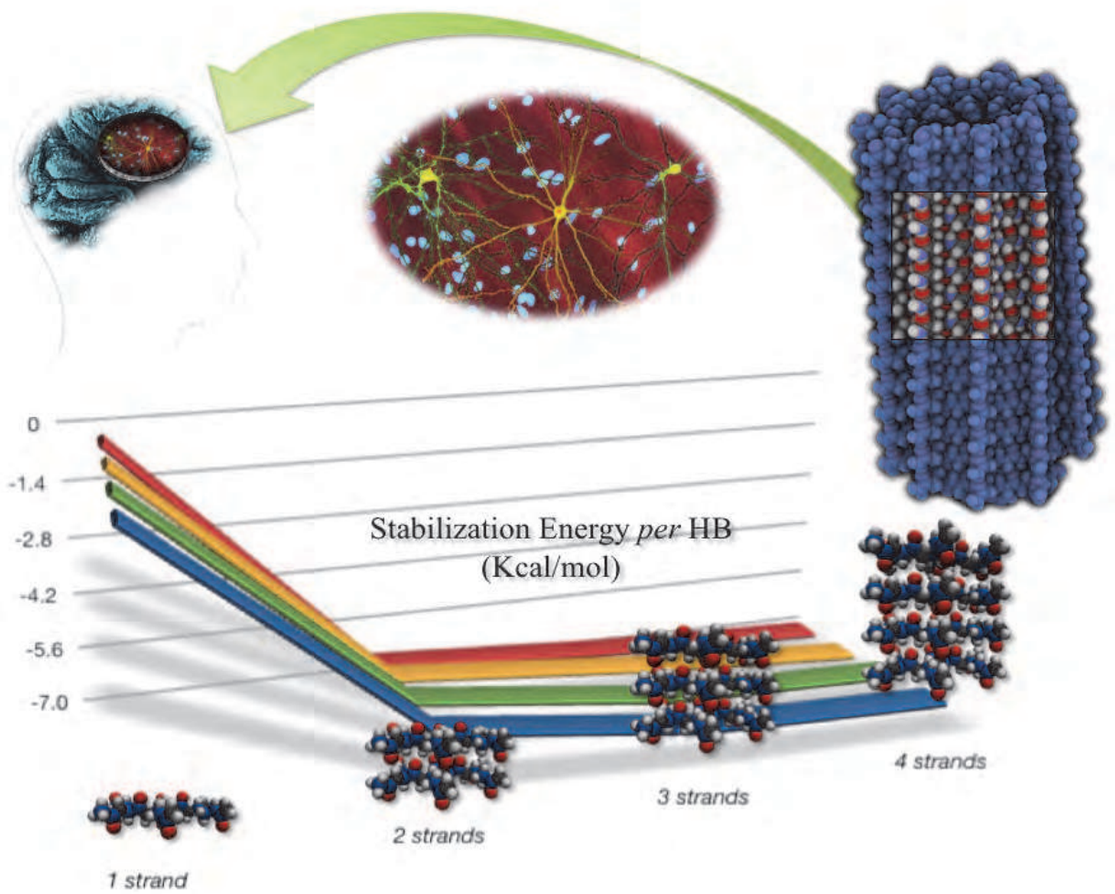

Fig. 6. Cooperative effect calculated as stabilization energy per H-bond.

3.3 Conformation of N17 in aqueous solution investigated by bias-exchange metadynamics

As stated in the introduction, recently, *in vivo* (Truant et al. 2008; Duennwald et al. 2006; Aiken et al. 2009), in cell (Ignatova et al. 2007; Cornett et al. 2005; Lakhani et al. 2010), *in vitro* (Rockabrand et al. 2007; Kim et al. 2009; Williamson et al. 2010) and *in silico* (Lakhani et al. 2010) studies showed that N17 modulates Htt fibrillation. This might arise by a variety of mechanisms, including changes in subcellular localization, nucleation of aggregation and/or interaction with cellular partners (Truant et al. 2008).

Understanding the influence of N17 on the aggregation mechanisms of polyQ in HD highly depends on structural information. Different spectroscopic techniques such as NMR (Thakur et al. 2009), CD (Thakur et al. 2009; Williamson et al. 2010) and FRET (Thakur et al. 2009) showed that N17 in aqueous solution adopts predominantly a random-coil structure with transient helical conformations (Thakur et al. 2009). Thus, N17 in solution can exist in equilibrium between different conformations. As these experimental techniques can provide only information on averages between the populations of different conformers, the secondary and the tertiary structure contents of the different N17 conformers remain not known. In this selected example (Rossetti G 2011) the Bias Exchange Metadynamics (BEM) was adopted to describe the thermodynamics and the kinetics of N17 in aqueous solution and at room temperature (Piana & Laio 2007). The BEM method relies on a combination of metadynamics and replica exchange. (Piana & Laio 2007; Laio & Gervasio 2008; Laio & Parrinello 2002). Metadynamics is a powerful algorithm used for accelerating rare events. In this scheme the system is described by a set of collective variables (CVs) and its normal evolution in the space of the CVs is biased by a history-dependent potential that forces the system to escape from local minima. This potential is, later, used to reconstruct the underlying free energy surface. Metadynamics, however, is effective only to explore few reaction coordinates as its performance decreases enormously with an increasing number of CVs. Typically, RE method is performed between replica of the system at different temperature as this latter is adopted to enhance the phase-space exploration (Piana et al. 2008; Sugita & Okamoto 2000). An example of RE metadynamics exists, in which a metadynamics run is performed in replicas of the system at different temperature (Bussi et al. 2006). However, in BEM exchanges are performed between replicas of the system at the same temperature, but using different CVs. This allows to extend the metadynamics approach to a virtually unlimited number of variables, becoming very effective for protein folding (Marinelli et al. 2009).

In this study BEM was employed to predict the free energy landscape of N17[k] in aqueous solution (Rossetti et al. 2008).[j] Our results showed that N17 populated four main kinetic basins, which interconverted on the second time-scale.[l] In each basin these were several possible clusters and an attractor, which was the lowest free energy cluster of the basin (Rossetti et al. 2011). The most populated basin (about 75%) was a random coil, with an extended flat exposed hydrophobic surface (B2, in Fig. 7). The latter may be crucial for the

[k]N17's extended coil conformation was built with the Modeller 9v8 program (Sánchez and Sali 1997). The D and K residues were considered to be in their ionized state.

[j]The first three (CV_1, CV_2, CV_3) count the number of hydrophobic contacts, of *C* contacts, and of backbone hydrogen bonds. CV_4 and CV_5 monitor the helical content in the whole and central part of the peptide. CV_6 is the dihedral correlation between successive dihedrals.

[l]The free energy of each cluster is estimated by a weighted-histogram approach (Kumar et al. 1992).

role of N17 in Htt oligomerization because such surface may create a hydrophobic seed around which the flanking polyQ tract can collapse (Truant et al. 2008; Ross & Tabrizi 2011; Ross et al. 2003) and promote hydrophobic-force driven associations between Htt N-terminal fragments (Thakur et al. 2009; Colby et al. 2004; Angeli et al. 2010; Tam et al. 2009). The other significantly populated basins, B1 and B3 (Fig. 7) assumed an amphipathic helical conformation, from residues 1 to 11 and from 1 to 7, respectively. Such conformation may

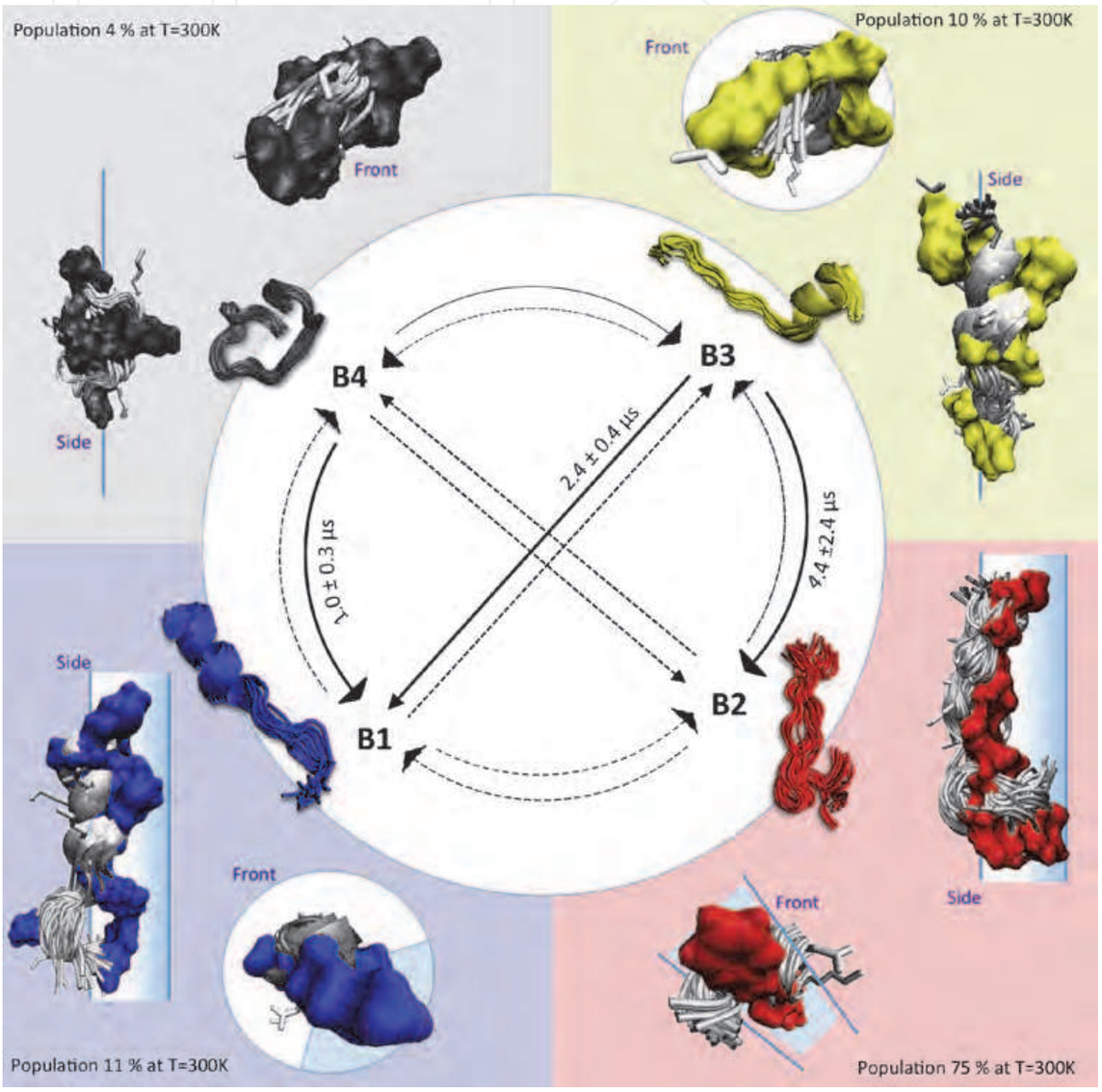

Fig. 7. The four basins (B1-B4) of N17 in aqueous solution. B1-B4 are characterized by their population and by their attractor. This latter is defined as the cluster with lowest free energy in the basin. Only the attractors' structures and their correspondent views of the hydrophobic side chain distribution are shown for clarity. The attractors' structures of B1 are colored in red, those of B2 in blue, those of B3 in yellow and those of B4 in grey. The calculated interconversion rates along with their corresponding statistical errors are reported. Dotted arrows are used for rates > 2 ms.

Modification	Q tract	In vivo	In cell	In vitro	Helix Propensity	Hydro phobicity	**SS pred**: secondary structure prediction **Burial_25:** burial, less than 25% solvent accesibility **Burial 5:** burial, less than 5% exposure **Reliability** of prediction accuracy, ranges from 0 to 9, bigger is better.
MATLEKLMKAFESLKSF	-	-	-	-	4.36	0.05	Sequence : MATLEKLMKAFESLKSF SS pred : - HHHHHHHHHHHHHHHHH Burial_25 : ---B--BB-BB--B--B Burial_5 : ------B---------- Reliability: 73799999999999998
MATAAAAAAAFESLKSF (Tam et al. 2009)	103	!	-	!	3.06	-0.09	Sequence : MATAAAAAAAFESLKSF SS pred : -- HHHHHHHHHHHHHHHH Burial_25 : ---B--BB-BB--B--B Burial_5 : ---------- Reliability: 98489999999999998
MATLEKPMPAFESLKSF (Tam et al. 2009)	103	-	-	!	0.22	-0.02	Sequence : MATLEKPMPAFESLKSF SS pred : ----------HHHHHHHH Burial_25 : ---B---B-BB--B--B Burial_5 : ---------- Reliability: 99846777746899998
Polar to A MATLAALMAAFESLKSF (Tam et al. 2009)	103	↓	-	↓	6.01	0.10	Sequence : MATLAALMAAFESLKSF SS pred : - HHHHHHHHHHHHHHHHH Burial_25 : ---BBBBBBB--B--B Burial_5 : ------B---------- Reliability: 73799999999999998
Non polar to A MATAEKAAKAFESLKSF (Tam et al. 2009)	103	!	-	↓	2.26	-0.14	Sequence : MATAEKAAKAFESLKSF SS pred : --- HHHHHHHHHHHHHHH Burial_25 : ---B--BB-BB--B--B Burial_5 : ---------- Reliability: 99768999999999998
MATLEKLMKAFEDLKDF *(Gu et al. 2009)*	97	↓	-	↓	4.31	-0.02	Sequence : MATLEKLMKAFEDLKDF SS pred : - HHHHHHHHHHHHHHHHH Burial_25 : ---B--BB-BB--B--B Burial_5 : ------B---------- Reliability: 73799999999999987
MAALEKLMKAFESLKSF *(Aiken et al. 2009)*	46	↓	↓	-	6.26	0.04	Sequence : MAALEKLMKAFESLKSF SS pred : -- HHHHHHHHHHHHHHHH Burial_25 : ---B--BB-BB--B--B Burial_5 : ------B---------- Reliability: 70899999999999987

↓ = decrease; ! = block; H=helix ; B = buried

Table 1. Bioinformatic calculations on N17. Calculated (Improta et al. 2001) helix propensity, hydrophobicity and number of buried residues of N17 and non-amyloidogenic mutants. In all calculations, pH, temperature and ionic strength were assumed to be the same as in the calculations, namely 7, 300K, 0.1M.

facilitate the binding on N17's target surface. This was consistent with the proposal that N17 assumes a helical fold by binding to a variety of cellular partners (Thakur et al. 2009; Colby et al. 2004; Angeli et al. 2010; Tam et al. 2009). This aspect, in turn, may have an impact on the formation of fibrils (Tam et al. 2009; Gu et al. 2009). The last basin B4 was characterized, instead, by a very small population and assumed a globular compact coiled structure. A variety of mutants of N17 are non-amyloidogenic (Tam et al. 2009; Gu et al. 2009). As for most of them, the mutation changes the nature of the residue from apolar to polar or vice versa, the result of the mutation is, probably, a reduction of the large content of amphiphatic conformations of N17 (Tam et al. 2009; Gu et al. 2009).[m] Consistently, the calculated folding propensity of these mutants differed significantly from that of N17 (Tab. 1). This hold true even if only a single point mutation was introduced (the N17(T3A) peptide) (Tam et al. 2009; Gu et al. 2009). In conclusion, changes in the relative population of the different basins induced by a change of amphiphaty may substantially affect the propensity of N17 mutants to form fibrils as observed experimentally (Rossetti et al. 2011).

4. Conclusions and perspectives

Our review clearly remarks the importance of computer simulations in complementing and interpreting experimental findings in neurodegenerative diseases. However, although computer simulations techniques are becoming more and more powerful to investigate these biological problems and the computer power continues to increase enormously, several aspects still limit the effective application of computational methods to a detailed understanding of the polyQ aggregation mechanism (Papaleo & Invernizzi 2011). The limited time scale accessible to full atomistic simulations requires the use of enhanced sampling algorithms to explore the conformational space of the folding and of the aggregation of Htt fragments, or to get insights into the physico-chemical determinants at the basis of this mechanism. However, these computational techniques are very demanding from the computational point of view and not yet capable of simulating the aggregation of long biologically relevant peptides. CG models may be suitable to study larger systems and to explore longer time scale than force filed based MD. However, they are lack of an atomistic description, which may be crucial to correctly describe the complex aggregation processes at the basis of neurodegenerative diseases. In this respect the development of accurate multiscale approaches based on a combination of CG and force field methods may be useful to overcome the limitations of both methodologies (Moroni et al. 2009; Tozzini 2010; Neri et al. 2005). From the experimental point of view, instead, limitations to a complete understanding of HD's onset mechanism are given by the lack of the crystallographic structure of the entire Htt protein, as well as by the lack of a detailed mapping of its interacting partners proteins. This latter aspect is becoming to be addressed both experimentally and computationally (Angeli et al. 2010; Rossetti et al. 2011). Moreover, theoretical and experimental studies demonstrated that several different aggregation pathways exist, resulting in different oligomeric and fibrillar structures of comparable stabilities. Probably, the dominant morphology of the aggregates is determined by the species having the lowest barrier to form the initial nucleation seed, rather than the largest

[m]The helix propensity, hydrophobicity and number of buried residues of N17 as well as those of the mutants in Tab 1 were estimated using the AGADIR ((Lacroix, et al. 1998) at http://agadir.crg.es/), PEPINFO (Sweet and Eisenberg 1983) at http://emboss.sourceforge.net/ and JPRED3 (Cole et al. 2008) at http://www.compbio.dundee.ac.uk/, respectively.

thermodynamic stability. However, the relative importance of kinetic and thermodynamics factors in amyloids grow is still a highly debated issue (Papaleo & Invernizzi 2011). Due to the increased potentialities of both experimental and computational approaches a synergistic effort should be immensely useful to unravel the toxicity mechanism of protein aggregation and, in particular, to further clarify several unclear aspects of the HD mechanism (Ma & Nussinov 2006; Miller et al. 2010). This may be also of help to identify and design specific molecules to hamper polyQ aggregation (Robertson & Bottomley 2010).

5. Acknowledgments

The authors thank Prof. P. Carloni, Dr. A. Pastore, Prof. F. Persichetti, Prof. A. Laio and P. Cossio as they have contributed to the selected applications presented here.

6. References

Aiken, C. T., J. S. Steffan, C. M. Guerrero, H. Khashwji, T. Lukacsovich, D. Simmons, J. M. Purcell, K. Menhaji, Y. Z. Zhu, K. Green, F. Laferla, L. Huang, L. M. Thompson, and J. L. Marsh. 2009. Phosphorylation of threonine 3: implications for Huntingtin aggregation and neurotoxicity. *J Biol Chem* 284 (43):29427-36. 1083-351X (Electronic) 0021-9258 (Linking).

Andrade, M. A., and P. Bork. 1995. Heat Repeats in the Huntingtons-Disease Protein. *Nature Genetics* 11 (2):115-116. 1061-4036.

Angeli, S., J. Shao, and M. I. Diamond. 2010. F-actin binding regions on the androgen receptor and huntingtin increase aggregation and alter aggregate characteristics. *PLoS ONE* 5 (2):e9053.

Armen, R. S., B. M. Bernard, R. Day, D. O. V. Alonso, and V. Daggett. 2005. Characterization of a possible amyloidogenic precursor in glutamine-repeat neurodegenerative diseases. *Proc Nat Acad Sci USA* 102 (38):13433-13438. 0027-8424.

Arrasate, M., S. Mitra, E. S. Schweitzer, M. R. Segal, and S. Finkbeiner. 2004. Inclusion body formation reduces levels of mutant huntingtin and the risk of neuronal death. *Nature* 431 (7010):805-810. 0028-0836.

Atwal, R. S., J. Xia, D.Pinchev, J. Taylor, R. M. Epand, and R. Truant. 2007. Huntingtin has a membrane association signal that can modulate huntingtin aggregation, nuclear entry and toxicity. *Hum Mol Gen* 16 (21):2600-15. Online ISSN 1460-2083 - Print ISSN 0964-6906.

Barton, S., R. Jacak, S. D. Khare, F. Ding, and N. V. Dokholyan. 2007. The length dependence of the polyQ-mediated protein aggregation. *J Biol Chem* 282 (35):25487-92. 0021-9258 (Print) 0021-9258 (Linking).

Bates, G. 2003. Huntingtin aggregation and toxicity in Huntington's disease. *Lancet* 361 (9369):1642-4. 0140-6736 (Print) 0140-6736 (Linking).

Bates, G. P., L. Mangiarini, and S. W. Davies. 1998. Transgenic Mice in the Study of Polyglutamine Repeat Expansion Diseases. *Brain Pathology* 8 (4):699-714. 1750-3639.

Beke, T., I. G. Csizmadia, and A. Perczel. 2006. Theoretical study on tertiary structural elements of beta-peptides: nanotubes formed from parallel-sheet-derived assemblies of beta-peptides. *J Am Chem Soc* 128 (15):5158-67. 0002-7863 (Print) 0002-7863 (Linking).

Benedek, N. A., I. K. Snook, K. Latham, and I. Yarovsky. 2005. Application of numerical basis sets to hydrogen bonded systems: a density functional theory study. *J Chem Phys* 122 (14):144102. 0021-9606 (Print).

Bennett, M. J., K. E. Huey-Tubman, A. B. Herr, A. P. West, S. A. Ross, and P. J. Bjorkman. 2002. A linear lattice model for polyglutamine in CAG-expansion diseases. *Proc Nat Acad Sci USA* 99 (18):11634-11639. 0027-8424.

Berendsen, H. J. C., D. van der Spoel, and R. van Drunen. 1995. GROMACS: a message-passing parallel molecular dynamics implementation. *Comput Phys Commun*.

Berman, H. 2000. The protein data bank: A retrospective and prospective. *Biophys J* 78 (1):267A-267A. 0006-3495.

Bhattacharyya, A. M., A. K. Thakur, and R. Wetzel. 2005. polyglutamine aggregation nucleation: thermodynamics of a highly unfavorable protein folding reaction. *Proc Natl Acad Sci U S A* 102 (43):15400-5. 0027-8424 (Print) 0027-8424 (Linking).

Bhattacharyya, A., A. K. Thakur, V. M. Chellgren, G. Thiagarajan, A. D. Williams, B. W. Chellgren, T. P. Creamer, and R. Wetzel. 2006. Oligoproline Effects on Polyglutamine Conformation and Aggregation. *J Mol Biol* 355 (3):524-535. 0022-2836.

Biarnes, X., S. Bongarzone, A. Vargiu, P. Carloni, and P. Ruggerone. 2011. Molecular motions in drug design: the coming age of the metadynamics method. *J Comput Aid Mol Des* 25 (5):395-402. 0920-654.

Borrell-Pages, M., D. Zala, S. Humbert, and F. Saudou. 2006. Huntington's disease: from huntingtin function and dysfunction to therapeutic strategies. *Cell Mol Life Sci* 63 (22):2642-2660. 1420-682.

Bulone, D., L.Masino, D. J. Thomas, P. L. San Biagio, and A. Pastore. 2006. The Interplay between PolyQ and Protein Context Delays Aggregation by Forming a Reservoir of Protofibrils. *PLoS ONE* 1 (1):e111.

Bussi, G., F. L. Gervasio, A. Laio, and M. Parrinello. 2006. Free-Energy Landscape for Œ≤ Hairpin Folding from Combined Parallel Tempering and Metadynamics. *J Am Chem Soc* 128 (41):13435-13441. 0002-7863.

Carloni, P., U. Rothlisberger, and M. Parrinello. 2002. The Role and Perspective of Ab Initio Molecular Dynamics in the Study of Biological Systems. *Accounts Chem Res* 35 (6):455-464. 0001-4842.

Caviston, J. P, J. L. Ross, S. M. Antony, M. Tokito, and E. L. F. Holzbaur. 2007. Huntingtin facilitates dynein/dynactin-mediated vesicle transport. *P Natl Acad Sci Usa* 104 (24):10045-50.

Cha, J.H. J. 2007. Transcriptional signatures in Huntington's disease. *Prog Neurobiol* 83 (4):228-48. 0301-0082.

Chen, S. M., V. Berthelier, J. B. Hamilton, B. O'Nuallain, and R. Wetzel. 2002. Amyloid-like features of polyglutamine aggregates and their assembly kinetics. *Biochem* 41 (23):7391-7399. 0006-2960.

Christ, C. D., A. E. Mark, and W. F. van Gunsteren. 2010. Basic ingredients of free energy calculations: A review. *J Comput Chem* 31 (8):1569-1582. 1096-987X.

Colby, D. W., Y.J. Chu, J.P. Cassady, M. Duennwald, H. Zazulak, J.M. Webster, A. Messer, S. Lindquist, V.M. Ingram, and K.D. Wittrup. 2004. Potent inhibition of huntingtin and cytotoxicity by a disulfide bond-free single-domain intracellular antibody. *Proc Nat Acad Sci USA* 101 (51):17616-17621.

Cole, C., J. D. Barber, and G. J. Barton. 2008. The Jpred 3 secondary structure prediction server. *Nucleic Acids Res* 36:W197-W201.

Cornett, J., F. Cao, C.E. Wang, C. A. Ross, G. P. Bates, S. H. Li, and X. J. Li. 2005. Polyglutamine expansion of huntingtin impairs its nuclear export. *Nat Genet* 37 (2):198-204.

CPMD 3.11.1. Copyright IBM Corp 1990-2008.

Davies, S. W., M. Turmaine, B. A. Cozens, M. DiFiglia, A.H. Sharp, C. A. Ross, E. Scherzinger, Erich E. Wanker, Laura Mangiarini, and Gillian P. Bates. 1997. Formation of Neuronal Intranuclear Inclusions Underlies the Neurological Dysfunction in Mice Transgenic for the HD Mutation. *Cell* 90 (3):537-548. 0092-8674.

Dehay, B., and A. Bertolotti. 2006. Critical role of the proline-rich region in Huntingtin for aggregation and cytotoxicity in yeast. *J Biol Chem* 281 (47):35608-35615.

Duennwald, M. L., S. Jagadish, P. J. Muchowski, and S. Lindquist. 2006. Flanking sequences profoundly alter polyglutamine toxicity in yeast. *Proc Nat Acad Sci USA* 103 (29):11045-11050.

Esposito, L., A. Paladino, C. Pedone, and L. Vitagliano. 2008. Insights into structure, stability, and toxicity of monomeric and aggregated polyglutamine models from molecular dynamics simulations. *Biophys J* 94 (10):4031-4040. 0006-3495.

Finke, J. M., and J. N. Onuchic. 2004. Simulations exploring the structural ensemble in the folding of proteins and amyloid peptides. Biophys J 86 (1):340A-340A. 0006-3495.

Finke, J. M., M. S. Cheung, and J. N. Onuchic. 2004. A Structural Model of Polyglutamine Determined from a Host-Guest Method Combining Experiments and Landscape Theory. *Biophys J* 87 (3):1900-1918. 0006-3495.

Grunewald, T., and M. F. Beal. 1999. Bioenergetics in Huntington's Disease. *Ann NY Acad Sci* 893 (1):203-213. 1749-6632.

Gu, X., E. R. Greiner, R. Mishra, R. Kodali, A. Osmand, S. Finkbeiner, J. S. Steffan, L. M. Thompson, R. Wetzel, and X. W. Yang. 2009. Serines 13 and 16 Are Critical Determinants of Full-Length Human Mutant Huntingtin Induced Disease Pathogenesis in HD Mice. *Neuron* 64 (6):828-840. 0896-6273.

Gunawardena, S., L.S. Her, R. G. Brusch, R. A. Laymon, I. R. Niesman, B. Gordesky-Gold, L. Sintasath, N. M. Bonini, and L. S. B. Goldstein. 2003. Disruption of Axonal Transport by Loss of Huntingtin or Expression of Pathogenic PolyQ Proteins in Drosophila. *Neuron* 40 (1):25-40. 0896-6273.

Gusella, J. F., and M. E. MacDonald. 2000. Molecular genetics: unmasking polyglutamine triggers in neurodegenerative disease. *Nat Rev Neurosci* 1 (2):109-15. 1474-1776.

Gutekunst, C. A., S. H. Li, H. Yi, J. S. Mulroy, S. Kuemmerle, R. Jones, D. Rye, R. J. Ferrante, S. M. Hersch, and X. J. Li. 1999. Nuclear and neuropil aggregates in Huntington's disease: Relationship to neuropathology. *J Neurosci* 19 (7):2522-2534. 0270-6474.

Hajime, O., N. Miki, W. Hirofumi, E. B. Starikov, M. Rothstein Stuart, and T. Shigenori. 2008. Molecular dynamics simulation study on the structural stabilities of polyglutamine peptides. *Comput Biol Chem* 32 (2):102-110. 1476-9271.

Harjes P., E.E. Wanker 2003. The hunt for huntingtin function: interaction partners tell many different stories. *Trends Biochem Sci* 28:425-433.

Horvath, V., Z. Varga, and A. Kovacs. 2004. Long-range effects in oligopeptides. A theoretical study of the beta-sheet structure of Gly(n) (n=2-10). *J Phys Chem A* 108 (33):6869-6873. 1089-5639.

Horvath V, Varga Z, Kovacs. 2005. Substituent effects on long-range interactions in the β-sheet structure of oligopeptides. *J. Mol. Struct. (Theochem.)* 755 (1-3):247-251. 0166-1280.

Housman, D. 1995. Gain of glutamines, gain of function? *Nat Genet* 10 (1):3-4. 1061-4036.

Huntington, G. 1872. On chorea. *The Medical and Surgical Reporter* 26 (15):317-321.

HyperChem 8.0, 1115 NW 4th St. Gainesville, FL 32608 (USA).

Ignatova, Z., A. K. Thakur, R. Wetzel, and L. M. Gierasch. 2007. In-cell aggregation of a polyglutamine-containing chimera is a multistep process initiated by the flanking sequence. *J Biol Chem* 282 (50):36736-43.

Imarisio, S., J. Carmichael, V. Korolchuk, C.W. Chen, S. Saiki, C. Rose, G. Krishna, J. E. Davies, E. Ttofi, B. R. Underwood, and D. C. Rubinsztein. 2008. Huntington's disease: from pathology and genetics to potential therapies. *Biochem J* 412 (2):191-209.

Improta, R., V. Barone, K. N. Kudin, and G. E. Scuseria. 2001. Structure and conformational behavior of biopolymers by density functional calculations employing periodic boundary conditions. I. The case of polyglycine, polyalanine, and poly-alpha-aminoisobutyric acid in vacuo. *J Am Chem Soc* 123 (14):3311-3322. 0002-7863.

Improta, R., and V. Barone. 2004. Assessing the reliability of density functional methods in the conformational study of polypeptides: The treatment of intraresidue nonbonding interactions. *J Comput Chem* 25 (11):1333-1341. 1096-987X.

Improta, R., V. Barone, K. N. Kudin, and G. E. Scuseria. 2001. The conformational behavior of polyglycine as predicted by a density functional model with periodic boundary conditions. *J Chem Phys* 114 (6):2541-2549. 0021-9606.

Johnson, C. D, and B. L. Davidson. 2010. Huntington's disease: progress toward effective disease-modifying treatments and a cure. *Hum Mol Genet* 19 (R1):R98-R102. Online 1460-2083 - Print 0964-6906.

Kaltenbach, L. S., E. Romero, R. R. Becklin, R. Chettier, R. Bell, A. Phansalkar, A. Strand, C. Torcassi, J. Savage, A. Hurlburt, G.H. Cha, L. Ukani, C.L. Chepanoske, Y. Zhen, S. Sahasrabudhe, J. Olson, C. Kurschner, L. M. Ellerby, J. M. Peltier, J. Botas, and R. E. Hughes. 2007. Huntingtin interacting proteins are genetic modifiers of neurodegeneration. *PLoS Genet* 3 (5):e82.

Kar, K., M. Jayaraman, B. Sahoo, R. Kodali, and R. Wetzel. 2011. Critical nucleus size for disease-related polyglutamine aggregation is repeat-length dependent. *Nat Struct Mol Biol*. 1545-9993.

Kegel, K. B., A. R. Meloni, Y. Yi, Y. J. Kim, E. Doyle, B. G. Cuiffo, E. Sapp, Y. Wang, Z.H. Qin, J. D. Chen, J. R. Nevins, N. Aronin, and M. DiFiglia. 2002. Huntingtin is present in the nucleus, interacts with the transcriptional corepressor C-terminal binding protein, and represses transcription. *J Biol Chem* 277 (9):7466-76. 0021-9258.

Kegel, K. B., E. Sapp, J. Yoder, B. Cuiffo, L. Sobin, Y. J. Kim, Z.H. Qin, M. R. Hayden, N. Aronin, D. L. Scott, G. Isenberg, W. H. Goldmann, and M. DiFiglia. 2005. Huntingtin associates with acidic phospholipids at the plasma membrane. *J Biol Chem* 280 (43):36464-73. 0021-9258.

Kelley, N. W., X. Huang, S. Tam, C. Spiess, J. Frydman, and V. S. Pande. 2009. The Predicted Structure of the Headpiece of the Huntingtin Protein and Its Implications on Huntingtin Aggregation. *J Mol Biol* 388 (5):919-927. 0022-2836.

Khare, S. D., F. Ding, K. N. Gwanmesia, and N. V. Dokholyan. 2005. Molecular origin of polyglutamine aggregation in neurodegenerative diseases. *PLoS Comp Biol* 1 (3):230-5.

Kim, M. W., Y. Chelliah, S. W. Kim, Z. Otwinowski, and I. Bezprozvanny. 2009. Secondary Structure of Huntingtin Amino-Terminal Region. *Structure (London, England : 1993)* 17 (9):1205-1212. 0969-2126.

Klein, F., A. Pastore, L. Masino, G. Zederlutz, H. Nierengarten, M. Ouladabdelghani, D. Altschuh, J. Mandel, and Y. Trottier. 2007. Pathogenic and Non-pathogenic Polyglutamine Tracts Have Similar Structural Properties: Towards a Length-dependent Toxicity Gradient. *J Mol Biol* 371 (1):235-244. 0022-2836.

Koch, O., M. Bocola, and G. Klebe. 2005. Cooperative effects in hydrogen-bonding of protein secondary structure elements: A systematic analysis of crystal data using Secbase. *Proteins: Struct, Fun, and Bio* 61 (2):310-317. 1097-0134.

Kuemmerle, S, C A Gutekunst, A M Klein, X J Li, S H Li, M F Beal, S M Hersch, and R J Ferrante. 1999. Huntington aggregates may not predict neuronal death in Huntington's disease. *Ann Neurol* 46 (6):842-9.

Kumar, S, D Bouzida, RH Swendsen, Peter A Kollman, and J.M. Rosenberg. 1992. THE weighted histogram analysis method for free-energy calculations on biomolecules.1. The Method. *J Comput Chem* 13 (8):1011-1021. 1096-987X.

Lacroix, E, A R Viguera, and L Serrano. 1998. Elucidating the folding problem of alpha-helices: local motifs, long-range electrostatics, ionic-strength dependence and prediction of NMR parameters. *J Mol Biol* 284 (1):173-91. 0022-2836.

Laghaei, R., and N. Mousseau. 2010. Spontaneous formation of polyglutamine nanotubes with molecular dynamics simulations. *J Chem Phys* 132 (16):165102. 0021-9606.

Laio, A., and F. L. Gervasio. 2008. Metadynamics: a method to simulate rare events and reconstruct the free energy in biophysics, chemistry and material science. *Rep Prog Phys* 71 (12):126601.

Laio, A., and M. Parrinello. 2002. Escaping free-energy minima. *P Natl Acad Sci Usa* 99 (20):12562-6.

Lakhani, Vinal V., Feng Ding, and Nikolay V. Dokholyan. 2010. Polyglutamine Induced Misfolding of Huntingtin Exon1 is Modulated by the Flanking Sequences. *PLoS Comput Biol* 6 (4):e1000772.

Leavitt, B. R., J. A. Guttman, J. G. Hodgson, G. H. Kimel, R. Singaraja, A. Wayne Vogl, and Michael R. Hayden. 2001. Wild-Type Huntingtin Reduces the Cellular Toxicity of Mutant Huntingtin In Vivo. *Am J Hum Genet* 68 (2):313-324. 0002-9297.

Leavitt, B. R., C. L. Wellington, and M. R. Hayden. 1999. Recent Insights into the Molecular Pathogenesis of Huntington Disease. *Semin Neurol* 19 (04):385,395. 0271-8235.

Lee, W.C. M., M. Yoshihara, and J. T. Littleton. 2004. Cytoplasmic aggregates trap polyglutamine-containing proteins and block axonal transport in a Drosophila model of Huntington's disease. *P Natl Acad Sci Usa* 101 (9):3224-9.

Legleiter, J., E. Mitchell, G. P. Lotz, E. Sapp, C. Ng, M. DiFiglia, L. M. Thompson, and P. J. Muchowski. 2010. Mutant huntingtin fragments form oligomers in a polyglutamine length-dependent manner in vitro and in vivo. *J Biol Chem* 285 (19):14777-90. 0021-9258.

Li, H, S H Li, Z X Yu, P Shelbourne, and X J Li. 2001. Huntingtin aggregate-associated axonal degeneration is an early pathological event in Huntington's disease mice. *J Neurosci* 21 (21):8473-81. 0270-6474.

Li, W., L. C. Serpell, W. J. Carter, D. C. Rubinsztein, and J. A. Huntington. 2006. Expression and characterization of full-length human huntingtin, an elongated HEAT repeat protein. *J Biol Chem* 281 (23):15916-22. 0021-9258.

Ma, B. and R. Nussinov. 2006. Simulations as analytical tools to understand protein aggregation and predict amyloid conformation. *Curr Opin Chem Biol* 10 (5):445-452. 1367-5931.

MacDonald, M. E., C. M. Ambrose, M. P. Duyao, R. H. Myers, C. Lin, L. Srinidhi, G. Barnes, S. A. Taylor, M. James, N. Groot, H. MacFarlane, B. Jenkins, M. A. Anderson, N. S. Wexler, J. F. Gusella, G. P. Bates, S. Baxendale, H. Hummerich, S. Kirby, M. North, S. Youngman, R. Mott, G. Zehetner, Z. Sedlacek, A. Poustka, A.M. Frischauf, H. Lehrach, A. J. Buckler, D. Church, L. Doucette-Stamm, M. C. O'Donovan, L. Riba-Ramirez, M. Shah, V. P. Stanton, S. A. Strobel, K. M. Draths, J. L. Wales, P. Dervan, D. E. Housman, M. Altherr, R. Shiang, L. Thompson, T. Fielder, J. J. Wasmuth, D. Tagle, J. Valdes, L. Elmer, M. Allard, L. Castilla, M. Swaroop, K. Blanchard, F. S. Collins, R. Snell, T. Holloway, K. Gillespie, N. Datson, D. Shaw, and P. S. Harper. 1993. A novel gene containing a trinucleotide repeat that is expanded and unstable on Huntington's disease chromosomes. *Cell* 72 (6):971-983. 0092-8674.

Mangiarini, L., K. Sathasivam, M. Seller, B. Cozens, A. Harper, C. Hetherington, M. Lawton, Y. Trottier, H. Lehrach, S. W. Davies, and G. P. Bates. 1996. Exon 1 of the HD gene with an expanded CAG repeat is sufficient to cause a progressive neurological phenotype in transgenic mice. *Cell* 87 (3):493-506. 0092-8674.

Marchut, A. J., and C. K. Hall. 2006a. Side-chain interactions determine amyloid formation by model polyglutamine peptides in molecular dynamics simulations. *Biophys J* 90 (12):4574-4584. 0006-3495.

Marchut A.J., C. K. Hall 2006b. Spontaneous formation of annular structures observed in molecular dynamics simulations of polyglutamine peptides. *Comput Biol Chem* 30 (3):215-218. 1476-9271.

Marchut A.J., C. K. Hall 2007. Effects of chain length on the aggregation of model polyglutamine peptides: Molecular dynamics simulations. *Proteins Struct Funct Bioinf* 66 (1):96-109. 0887-3585.

Marinelli, F., F. Pietrucci, A. Laio, and S. Piana. 2009. A kinetic model of trp-cage folding from multiple biased molecular dynamics simulations. *PLoS Comp Biol* 5 (8):e1000452.

Masino, L., G. Kelly, K. Leonard, Y. Trottier, and A. Pastore. 2002. Solution structure of polyglutamine tracts in GST-polyglutamine fusion proteins. *Febs Lett* 513 (2-3):267-272. 0014-5793.

Merlino, A., L. Esposito, and L. Vitagliano. 2006. Polyglutamine repeats and beta-helix structure: Molecular dynamics study. *Proteins Struct Funct Bioinf* 63 (4):918-927. 0887-3585.

Miller, Y., B. Ma, and R. Nussinov. 2010. Polymorphism in Alzheimer A beta Amyloid Organization Reflects Conformational Selection in a Rugged Energy Landscape. *Chem Rev* 110 (8):4820-4838. 0009-2665.

Morley, J. F., H. R. Brignull, J. J. Weyers, and R. I. Morimoto. 2002. The threshold for polyglutamine-expansion protein aggregation and cellular toxicity is dynamic and influenced by aging in Caenorhabditis elegans. *Proc Nat Acad Sci USA* 99 (16):10417-10422. 0027-8424.

Moroni, E., G. Scarabelli, and G. Colombo. 2009. Structure and sequence determinants of aggregation investigated with molecular dynamics. *Front Biosci* 14:523-539. 1093-4715.

Morozov, A. V., T. Kortemme, K. Tsemekhman, and D. Baker. 2004. Close agreement between the orientation dependence of hydrogen bonds observed in protein structures and quantum mechanical calculations. *Proc Natl Acad Sci U S A* 101 (18):6946-51. 0027-8424 (Print).

Myers, R. 2004. Huntington's Disease Genetics. *NeuroRX* 1 (2):255-262.

Nagai, Y., T. Inui, H. A. Popiel, N. Fujikake, K. Hasegawa, Y. Urade, Y. Goto, H. Naiki, and T. Toda. 2007. A toxic monomeric conformer of the polyglutamine protein. *Nat Struct Mol Biol* 14 (4):332-340. 1545-9993.

Neri, M., C. Anselmi, M. Cascella, A. Maritan, and P. Carloni. 2005. Coarse-grained model of proteins incorporating atomistic detail of the active site. *Phys Rev Lett* 95 (21):218102.

Ogawa, H., M. Nakano, H. Watanabe, E. B. Starikov, S. M. Rothstein, and S. Tanaka. 2008. Molecular dynamics simulation study on the structural stabilities of polyglutamine peptides. *Comput Biol Chem* 32 (2):102-110. 1476-9271.

Olshina, M A, L M Angley, Y M Ramdzan, J Tang, M F Bailey, A F Hill, and D M Hatters. 2010. Tracking Mutant Huntingtin Aggregation Kinetics in Cells Reveals Three Major Populations That Include an Invariant Oligomer Pool. *J Biol Chem* 285 (28):21807-21816. 0021-9258.

Oma, Y., Y. Kino, N. Sasagawa, and S. Ishiura. 2004. Intracellular localization of homopolymeric amino acid-containing proteins expressed in mammalian cells. *J Biol Chem* 279 (20):21217-22. 0021-9258.

Palidwor, G. A, S. Shcherbinin, M. R. Huska, T. Rasko, U. Stelzl, A. Arumughan, R. Foulle, P. Porras, L. Sanchez-Pulido, E. E. Wanker, and M. A. Andrade-Navarro. 2009. Detection of alpha-rod protein repeats using a neural network and application to huntingtin. *PLoS Comp Biol* 5 (3):e1000304.

Papaleo, E., and G. Invernizzi. 2011. Conformational Diseases: Structural Studies of Aggregation of Polyglutamine Proteins. *Curr Comput-Aid Drug*. no. 7 (1):23-43.

Parker, J A, J B Connolly, C Wellington, M Hayden, J Dausset, and C Neri. 2001. Expanded polyglutamines in Caenorhabditis elegans cause axonal abnormalities and severe dysfunction of PLM mechanosensory neurons without cell death. *P Natl Acad Sci Usa* 98 (23):13318-23.

Perczel, A., Z. Gaspari, and I. G. Csizmadia. 2005. Structure and stability of beta-pleated sheets. *J Comput Chem* 26 (11):1155-1168. 1096-987X.

Perdew, J. P., K. Burke, and M. Ernzerhof. 1996. Generalized Gradient Approximation Made Simple. *Phys Rev Lett* 77 (18):3865-3868. 0031-9007 (Print).

Perutz, M. 1994. Polar Zippers - Their Role in Human-Disease. *Protein Sci* 3 (10):1629-1637. 0961-8368.

Perutz, M. F. 1999. Glutamine repeats and neurodegenerative diseases: molecular aspects. *Trends Biochem Sci* 24 (2):58-63. 0968-0004.

Perutz, M. F., J. T. Finch, J. Berriman, and A. Lesk. 2002. Amyloid fibers are water-filled nanotubes. *Proc Nat Acad Sci USA* 99 (8):5591-5595.

Perutz, M. F., and A. H. Windle. 2001. Cause of neural death in neurodegenerative diseases attributable to expansion of glutamine repeats. *Nature* 412 (6843):143-144. 0028-0836.

Piana, S, and A. Laio. 2007. A Bias-Exchange Approach to Protein Folding. *J Phys Chem B* 111 (17):4553-4559. 1520-6106.

Piana, S., A. Laio, F. Marinelli, M. Van Troys, D. Bourry, C. Ampe, and J. C. Martins. 2008. Predicting the Effect of a Point Mutation on a Protein Fold: The Villin and Advillin Headpieces and Their Pro62Ala Mutants. *J Mol Biol* 375 (2):460-470. 0022-2836.

Raetz, C. R. H., and S. L. Roderick. 1995. A Left-Handed Parallel beta Helix in the Structure of UDP-N-Acetylglucosamine Acyltransferase. *Science* 270 (5238):997-1000. 0036-8075.

Ramdzan, Y. M., R. M. Nisbet, J. Miller, S. Finkbeiner, A. F. Hill, and D. M. Hatters. 2010. Conformation Sensors that Distinguish Monomeric Proteins from Oligomers in Live Cells. *Chem. & Biol* 17 (4):371-379. 1074-5521.

Reiner, Anton, Ioannis Dragatsis, Scott Zeitlin, and Daniel Goldowitz. 2003. Wild-type huntingtin plays a role in brain development and neuronal survival. *Mol Neurobiol* 28 (3):259-275. 0893-7648.

Robertson, A. L., and S. P. Bottomley. 2010. Towards the Treatment of Polyglutamine Diseases: The Modulatory Role of Protein Context. *Curr Med Chem* 17 (27):3058-3068. 0929-8673.

Rockabrand, E., N. Slepko, A. Pantalone, V. N Nukala, A. G. Kazantsev, J. L. Marsh, P. G. Sullivan, J. S. Steffan, S. L. Sensi, and L. M. Thompson. 2007. The first 17 amino acids of Huntingtin modulate its sub-cellular localization, aggregation and effects on calcium homeostasis. *Hum Mol Gen* 16 (1):61-77. 0964-6906.

Rohrig, U. F., A. Laio, N. Tantalo, M. Parrinello, and R. Petronzio. 2006. Stability and structure of oligomers of the Alzheimer peptide A beta(16-22): From the dimer to the 32-mer. *Biophys J* 91 (9):3217-3229. 0006-3495.

Ross, C. A., and M. A. Poirier. 2004. Protein aggregation and neurodegenerative disease. *Nature Med*:S10-S17. 1078-8956.

Ross, C. 1995. When more is less: Pathogenesis of glutamine repeat neurodegenerative diseases. *Neuron* 15 (3):493-496. 0896-6273.

Ross, C. A, M. A. Poirier, E. E. Wanker, and Mario Amzel. 2003. Polyglutamine fibrillogenesis: The pathway unfolds. *Proc Nat Acad Sci USA* 100 (1):1-3.

Ross, C. A., and S. J. Tabrizi. 2011. Huntington's disease: from molecular pathogenesis to clinical treatment. *Lancet Neurol* 10 (1):83-98. 1474-4422.

Ross, C., and M. Poirier. 2005. What is the role of protein aggregation in neurodegeneration? *Nature Rev Mol Cell Biol* 6 (11):891-898. 1471-0072.

Rossetti G, Angeli S, Magistrato A, Diamod M, Carloni P. 2011. Actin binding by Htt blocks intracellular aggregation. *sumitted to Plos One*.

Rossetti, G:, Pilar C:, A. Laio, and P. Carloni. 2011. Conformations of the Huntingtin N-term in aqueous solution from atomistic simulations. *Febs Letters* 585 (19):3086-3089. 0014-5793.

Rossetti, G., A. Magistrato, A. Pastore, and P. Carloni. 2010. Hydrogen Bonding Cooperativity in polyQ beta-Sheets from First Principle Calculations. *J Chem Theory Comput* 6 (6):1777-1782. 1549-9618.

Rossetti, G., A. Magistrato, A. Pastore, F. Persichetti, and P. Carloni. 2008. Structural Properties of Polyglutamine Aggregates Investigated via Molecular Dynamics Simulations. *J Phys Chem B* 112 (51):16843-16850. 1520-6106.

Sánchez, R, and A Sali. 1997. Evaluation of comparative protein structure modeling by MODELLER-3. *Proteins* Suppl 1:50-8.

Sapp, E., J. Penney, A. Young, N. Aronin, J. P. Vonsattel, and M. DiFiglia. 1999. Axonal transport of N-terminal huntingtin suggests early pathology of corticostriatal projections in Huntington disease. *J Neuropathol Exp Neurol* 58 (2):165-173. 0022-3069.

Saudou, F., S. Finkbeiner, D. Devys, and M. E. Greenberg. 1998. Huntingtin Acts in the Nucleus to Induce Apoptosis but Death Does Not Correlate with the Formation of Intranuclear Inclusions. *Cell* 95 (1):55-66. 0092-8674.

Scheiner, S., and T. Kar. 2005. Effect of Solvent upon CH...O Hydrogen Bonds with Implications for Protein Folding. *J Phys Chem B* 109 (8):3681-3689. 1520-6106.

Sharma, D., L. M. Shinchuk, H. Inouye, R. Wetzel, and D. A. Kirschner. 2005. Polyglutamine homopolymers having 8-45 residues form slablike beta-crystallite assemblies. *Proteins Struct Funct Bioinf* 61 (2):398-411. 0887-3585.

Sikorski, P., and E. Atkins. 2005. New model for crystalline polyglutamine assemblies and their connection with amyloid fibrils. *Biomacromolecules* 6 (1):425-432. 1525-7797.

Spiegel, K., and A. Magistrato. 2006. Modeling anticancer drug-DNA interactions via mixed QM/MM molecular dynamics simulations. *Org Biomol Chem* 4 (13):2507-2517. 1477-0520.

Steffan, J. S, N. Agrawal, J. Pallos, E. Rockabrand, L. C Trotman, N. Slepko, K. Illes, T. Lukacsovich, Y.Z. Zhu, E. Cattaneo, P. P. Pandolfi, L. M. Thompson, and J. L. Marsh. 2004. SUMO modification of Huntingtin and Huntington's disease pathology. *Science* 304 (5667):100-4. 0036-8075.

Stork, M., A. Giese, H. A. Kretzschmar, and P. Tavan. 2005. Molecular dynamics simulations indicate a possible role of parallel beta- helices in seeded aggregation of poly-Gln. *Biophys J* 88 (4):2442-2451. 0006-3495.

Strehlow, A. N. T., J. Z Li, and R. M. Myers. 2007. Wild-type huntingtin participates in protein trafficking between the Golgi and the extracellular space. *Hum Mol Genet* 16 (4):391-409. 1460-2083.

Sugaya, K., S. Matsubara, Y. Kagamihara, A. Kawata, and H. Hayashi. 2007. Polyglutamine Expansion Mutation Yields a Pathological Epitope Linked to Nucleation of Protein Aggregate: Determinant of Huntington's Disease Onset. *PLoS ONE* 2 (7):e635.

Sugita, Y., and Y. Okamoto. 2000. Replica-exchange multicanonical algorithm and multicanonical replica-exchange method for simulating systems with rough energy landscape. *Chem Phys Lett* 329 (3-4):261-270. 0009-2614.

Sunde, M., and C. Blake. 1997. The structure of amyloid fibrils by electron microscopy and X-ray diffraction. *Adv Protein Chem* 50:123-159. 0065-3233.

Sunde, M., L. C. Serpell, M. Bartlam, P. E. Fraser, M. B. Pepys, and C. C. F. Blake. 1997. Common core structure of amyloid fibrils by synchrotron X-ray diffraction. *J Mol Biol* 273 (3):729-739. 0022-2836.

Sweet, R. M., and D. Eisenberg. 1983. Correlation of sequence hydrophobicities measures similarity in three-dimensional protein structure. *J Mol Biol* 171 (4):479-488. 0022-2836.

Tam, S., C. Spiess, W. Auyeung, L. Joachimiak, B. Chen, M. A. Poirier, and J. Frydman. 2009. The chaperonin TRiC blocks a huntingtin sequence element that promotes the conformational switch to aggregation. *Nat Struct Mol Biol* 16 (12):1279-1285. 1545-9993.

Tanaka, M., I. Morishima, T. Akagi, T. Hashikawa, and N. Nukina. 2001. Intra- and intermolecular beta-pleated sheet formation in glutamine-repeat inserted myoglobin as a model for polyglutamine diseases. *J Biol Chem* 276 (48):45470-45475. 0021-9258.

Tartari, Marzia, Carmela Gissi, Valentina Lo Sardo, Chiara Zuccato, Ernesto Picardi, Graziano Pesole, and Elena Cattaneo. 2008. Phylogenetic comparison of huntingtin homologues reveals the appearance of a primitive polyQ in sea urchin. *Mol Biol Evol* 25 (2):330-8. 1537-1719.

Thakur, A. K., M. Jayaraman, R. Mishra, M. Thakur, V. M. Chellgren, I.J. L. Byeon, D. H. Anjum, R. Kodali, T. P. Creamer, J. F. Conway, A. M. Gronenborn, and R. Wetzel. 2009. Polyglutamine disruption of the huntingtin exon 1 N terminus triggers a complex aggregation mechanism. *Nat Struct Mol Biol* 16 (4):380-389. 1545-9993.

Tozzini, V. 2010. Multiscale Modeling of Proteins. *Accounts Chem Res*. no. 43 (2):220-230. doi: 10.1021/ar9001476

Trottier, Y., Y. Lutz, G. Stevanin, G. Imbert, D. Devys, G. Cancel, F. Saudou, C. Weber, G. David, L. Tora, Y. Agid, A. Brice, and J. L. Mandel. 1995. Polyglutamine Expansion as a Pathological Epitope in Huntingtons-Disease and 4 Dominant Cerebellar Ataxias. *Nature* 378 (6555):403-406. 0028-0836.

Truant, R., R. S. Atwal, C. Desmond, L. Munsie, and T. Tran. 2008. Huntington's disease: revisiting the aggregation hypothesis in polyglutamine neurodegenerative diseases. *FEBS J* 275 (17):4252-4262. 1742-4658.

Tsemekhman, K., L. Goldschmidt, D. Eisenberg, and D. Baker. 2007. Cooperative hydrogen bonding in amyloid formation. *Protein Sci* 16 (4):761-764. 1469-896X.

van der Spoel, D., E. Lindahl, B. Hess, G. Groenhof, A. E. Mark, and H. J. Berendsen. 2005. GROMACS: Fast, flexible, and free. *J Comput Chem* 26 (16):1701-1718. 1096-987X.

Varga, Z., and A. Kovács. 2005. Hydrogen bonding in peptide secondary structures. *Int J Quantum Chem* 105 (4):302-312. 1097-461X.

Viswanathan, R., A. Asensio, and J. J. Dannenberg. 2004. Cooperative Hydrogen-Bonding in Models of Antiparallel b-Sheets. *J Phys Chem A* 108 (42):9205-9212. 1089-5639.

Vitalis, A., N. Lyle, and R. V. Pappu. 2009. Thermodynamics of ≤-Sheet Formation in Polyglutamine. *Biophys J* 97 (1):303-311. 0006-3495.

Wanker, E E. 2000. Protein aggregation and pathogenesis of Huntington's disease: mechanisms and correlations. *Biol Chem* 381 (9-10):937-942. 1431-6730.

Wieczorek, R., and J. J. Dannenberg. 2003. H-bonding cooperativity and energetics of alpha-helix formation of five 17-amino acid peptides. *J Am Chem Soc* 125 (27):8124-9. 0002-7863 (Print).

Williamson, T. E., An. Vitalis, S. L. Crick, and R. V. Pappu. 2010. Modulation of Polyglutamine Conformations and Dimer Formation by the N-Terminus of Huntingtin. *J Mol Biol* 396 (5):1295-1309. 0022-2836.

Zanuy, D., K. Gunasekaran, A. M. Lesk, and R. Nussinov. 2006. Computational study of the fibril organization of polyglutamine repeats reveals a common motif identified in beta-helices. *J Mol Biol* 358 (1):330-345. 0022-2836.

Zhao, Y. L., and Y. D. Wu. 2002. A theoretical study of beta-sheet models: is the formation of hydrogen-bond networks cooperative? *J Am Chem Soc* 124 (8):1570-1. 0002-7863.

Zhou, Z., J. Zhao, H. Liu, J. W. Wu, K. Liu, C. Chuang, W. Tsai, and Y. Ho. 2011. The Possible Structural Models for Polyglutamine Aggregation: A Molecular Dynamics Simulations Study. *J Biomol Struct Dyn* 28 (5):743-758. 0739-1102.

Zoghbi, H. Y., and H. T. Orr. 2000. Glutamine repeats and neurodegeneration. *Annu Rev Neurosci* 23:217-247.

Zuccato, C, M Valenza, and E. Cattaneo. 2010. Molecular Mechanisms and Potential Therapeutical Targets in Huntington's Disease. *Phys Rev* 90 (3):905-981.

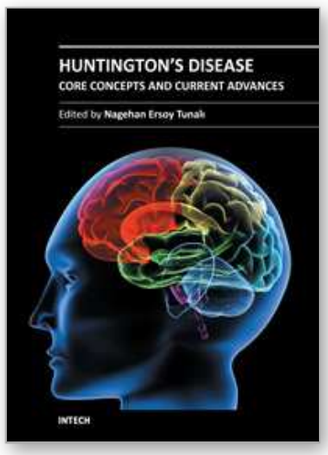

Huntington's Disease - Core Concepts and Current Advances
Edited by Dr Nagehan Ersoy Tunali

ISBN 978-953-307-953-0
Hard cover, 554 pages
Publisher InTech
Published online 15, February, 2012
Published in print edition February, 2012

Huntington's Disease is one of the well-studied neurodegenerative conditions, a quite devastating and currently incurable one. It is a brain disorder that causes certain types of neurons to become damaged, causing various parts of the brain to deteriorate and lose their function. This results in uncontrolled movements, loss of intellectual capabilities and behavioural disturbances. Since the identification of the causative mutation, there have been many significant developments in understanding the cellular and molecular perturbations. This book, "Huntington's Disease - Core Concepts and Current Advances", was prepared to serve as a source of up-to-date information on a wide range of issues involved in Huntington's Disease. It will help the clinicians, health care providers, researchers, graduate students and life science readers to increase their understanding of the clinical correlates, genetic aspects, neuropathological findings, cellular and molecular events and potential therapeutic interventions involved in HD. The book not only serves reviewed fundamental information on the disease but also presents original research in several disciplines, which collectively provide comprehensive description of the key issues in the area.

How to reference
In order to correctly reference this scholarly work, feel free to copy and paste the following:

Giulia Rossetti and Alessandra Magistrato (2012). Molecular Mechanism of Huntington’s Disease — A Computational Perspective, Huntington's Disease - Core Concepts and Current Advances, Dr Nagehan Ersoy Tunali (Ed.), ISBN: 978-953-307-953-0, InTech, Available from: http://www.intechopen.com/books/huntington-s-disease-core-concepts-and-current-advances/molecular-mechanism-of-huntington-s-disease-a-computational-perspective

INTECH
open science | open minds

InTech Europe
University Campus STeP Ri
Slavka Krautzeka 83/A
51000 Rijeka, Croatia
Phone: +385 (51) 770 447
Fax: +385 (51) 686 166
www.intechopen.com

InTech China
Unit 405, Office Block, Hotel Equatorial Shanghai
No.65, Yan An Road (West), Shanghai, 200040, China
中国上海市延安西路65号上海国际贵都大饭店办公楼405单元
Phone: +86-21-62489820
Fax: +86-21-62489821

IntechOpen